UC Berkeley
UC Berkeley Electronic Theses and Dissertations

Title

Autophagy and cellular signaling: a two-way relationship

Permalink

https://escholarship.org/uc/item/0sg013cs

Author

Segura-Roman, Ashley

Publication Date

2024

Supplemental Material

https://escholarship.org/uc/item/0sg013cs#supplemental

Peer reviewed|Thesis/dissertation

Autophagy and Cellular Signaling: A Two-Way Relationship

By

Ashley Segura-Roman

A dissertation submitted in partial satisfaction of the

requirements for the degree of

Doctor of Philosophy

in

Molecular and Cell Biology

in the

Graduate Division

of the

University of California, Berkeley

Committee in charge:

Professor Roberto Zoncu, Chair
Professor Micha Rape
Professor James Olzmann
Professor James Hurley

Summer 2024

Abstract

Autophagy and Cellular Signaling: A Two-Way Relationship

By

Ashley Segura-Roman

Doctor of Philosophy in Molecular and Cell Biology

University of California, Berkeley

Professor Roberto Zoncu, Chair

The correct function of organisms ranging from bacteria to humans critically depends on the cells' ability to rapidly change its metabolism through dedicated signaling cascades that transduce signals present in the surrounding environment. Two examples of these signaling cascades: mechanistic target of rapamycin complex 1 (mTORC1) and cAMP-dependent protein kinase A (PKA) work in tangent with cellular processes like autophagy to maintain cellular homeostasis. The two-way regulation between mTORC1 and autophagy is clear but the relationship between autophagy and PKA is more complex. Here I will focus on this complex interaction and propose a model where autophagy is regulating the PKA holoenzyme but also becomes a signaling scaffold for AKAP11-bound PKA. Furthermore, I also talk about the implications of our findings in the context of schizophrenia and bipolar disorder.

1

ACKOWLEDGEMENTS

Table of contents

Chapter 1: Introduction to cellular signaling by mTORC1 and PKA and their maintenance of cellular homeostasis

Chapter 2: AKAP11 coordinates an autophagy-dependent regulatory checkpoint that shapes neuronal PKA signaling

List of Figures

Chapter 1

1.1 Cellular Homeostasis Background and Significance

The correct function of organisms, ranging from bacteria to humans, critically depends on the cells' ability to rapidly change its metabolism through dedicated signaling cascades that transduce signals present in the surrounding environment. Activation of signaling cascades help rebalance the biochemical processes within the cell, playing a crucial role in maintaining cellular homeostasis. Two examples of these types of signaling pathways are mechanistic target of rapamycin complex 1 (mTORC1) and cAMP-dependent protein kinase A (PKA).

1.1.1 mTORC1

The Ser/Thr kinase mTOR is part of the larger signaling complex mTORC1 that integrates signals on the status of energy and nutrients, sensing nutrient levels, growth factors, energy sources and oxygen, coordinating the synthesis or breakdown of new cellular components. It plays a large role in the organization of both cellular and organismal physiology and is central to all eukaryotes.

In cells, abundance of nutrients (signal of pro-growth) corresponds to the activation of mTORC1. Phosphorylation of mTOR substrates carefully activates anabolic process while limiting autophagic processes or cellular breakdown (Saxton & Sabatini, 2017; Valvezan & Manning, 2019). Activation of mTORC1 requires localization from the cytoplasm to the lysosome where it can phosphorylate down-stream substrates. A large activity of mTORC1 activation is to upregulate protein synthesis by promoting translation initiation via the inhibition of 4EBP1 and activation of S6K1 (Brunn et al., 1997; Gingras et al., 1999; Kuo et al., 1992). But mTORC1 activity also promotes the production of building blocks that are required for cell growth, like nucleotide synthesis (Ben-Sahra et al., 2013, 2016; Robitaille et al., 2013) and lipogenesis (Düvel et al., 2010; Porstmann et al., 2008). Given that mTORC1 promotes the synthesis of cellular building blocks, it is also true that mTORC1 is highly sensitive to the depletion of these macromolecules, i.e. amino acids, nucleic acids, nucleotides, glucose. When these macromolecules are depleted, mTORC1 is unable to stimulate the downstream anabolic processes. Instead, the repression of mTORC1, due to unavailability of macromolecules, induces the autophagic turnover of macromolecules back to their building blocks (Valvezan & Manning, 2019). This careful coordination between anabolic

and catabolic programs, mediated by mTORC1, is how nutrient homeostasis is, in-part, maintained.

In disease, this need for careful tuning is further highlighted as dysregulated mTORC1 is central to many diseases. Chronic mTORC1 activation has been implicated in diseases such as cancers, obesity and type 2 diabetes, neurological disorders, as well as autoimmune diseases (S. C. Johnson et al., 2013; Saxton & Sabatini, 2017; Valvezan & Manning, 2019).

1.1.2 PKA

cAMP-dependent protein kinase (PKA), a Ser/Thr kinase, is a key protein kinase that regulates critical pathways for growth, development and response to stress (Taylor et al., 2013). PKA integrates cyclic adenosine monophosphate (cAMP)-mediated signals as a function of cellular state. Inactive PKA exists as a tetrameric holoenzyme, with two regulatory subunits bound to two catalytic subunits (Hilger et al., 2018). PKA activity is tightly regulated by the concentration of cyclic adenosine 3'5' monophosphate (cAMP). cAMP is an important second messenger, involved in diverse metabolic pathways such as regulation of glucose homeostasis, fat metabolism and cold adaptation (Krebs, 1989).

PKA signaling occurs first through the activation of G-protein coupled receptors (GPCRs). GPCRs integrate extracellular signals and are activated by signals like hormones, neurotransmitters, chemokines and odorants. This activation is then translated within the cell through the production of cAMP (Rehman et al., 2024). cAMP is produced by adenyl cyclases. Levels of cAMP are tightly coordinated by the production (by adenyl cyclase) and breakdown (by phosphodiesterases). Once activated, PKA phosphorylates a wide variety of proteins including ion channels, enzymes, and transcription factors.

In the regulation of PKA activity, increased concentrations of cAMP bind the regulatory subunit of PKA, of which there are two classes (RI and RII) each with two isoforms (α and β), inducing a conformational change releasing the catalytic subunit and phosphorylating a variety of substrates (Skalhegg & Tasken, 2000; Taskén & Aandahl, 2004). However, recently a new model is proposed in which binding of cAMP to the regulatory subunit of PKA does not fully release the catalytic subunit but rather causes an unhinging of the catalytic subunit from the regulatory subunit that spatially restricts the catalytic subunit but still promotes phosphorylation of PKA substrates (Omar & Scott, 2020).

To further restrict PKA signaling, spatially and temporally, PKA associates with tethering proteins called A kinase anchoring proteins (AKAPs) to form microdomains at specific subcellular localizations (Lefkimmiatis & Zaccolo, 2014). Microdomains

containing AKAP and PKA form functional signalosomes as they also house PKA substrates as well as other PKA signal regulators (phosphatases and phosphodiesterases) to further spatially and temporally restrict PKA signaling (Kritzer et al., 2012; McConnachie et al., 2006).

The tight regulation and coordination of PKA is necessary and can be appreciated through the effects in diseases that fundamentally have dysregulation in PKA itself. Two of these diseases, Carney Complex (CNC) and acrodysostosis-1 (ACRDYS1), are linked to the PRKAR1a gene but have contrasting phenotypes (Bruystens et al., 2016). While mutations of CNC cause increased PKA activity; the mutations in ACRDYS1 result in decreased PKA activity. Structure analysis of the PKA R1a protein shows that ACRDYS1 mutations are primarily found within the CNB-B domain, one of the two cAMP binding domains. These mutations render PKA holoenzymes that become resistant to cAMP. Additionally, the mutations also strengthen the RIa-C interaction. (Bruystens et al., 2016).

Strengthening the Ria and C interaction outside of a disease context seems to be a reoccurring theme to regulate PKA signaling. There are multiple serines surrounding the inhibitory site of RIa, that when phosphorylated by other kinases, modulate the degree of activation of PKA when stimulated by cAMP(Boeshans et al., 1999; Gupte et al., 2006; Han et al., 2013; Haushalter et al., 2018). In chapter 2, we identify ser83 as phosphorylated in an AKAP11-dependent manner and further characterize PKA activation in a phosphomimetic mutant.

1.2 Process of Autophagy in maintaining homeostasis

Macroautophagy (hereafter autophagy) is a vesicular catabolic process in which proteins, macromolecules and organelles are captured within a double-membraned organelle called the autophagsome. The cargo captured by the autophagosome is delivered to the lysosome through fusion of the outer membranes, creating the auto-lysosome. By this process, hydrolases, such as lipases, proteases, nucleases and glycosylases, found within the lysosome are shared to degrade the autophagic cargo (Nakatogawa, 2020; Yamamoto et al., 2023).

1. Formation   2. Fusion   3. Autolysosome
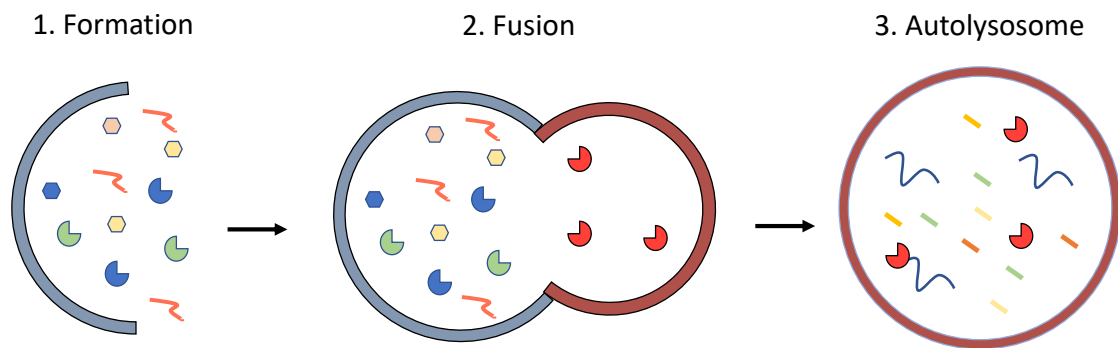
Autophagy for a long time was thought to be only a 'non-selective' process, where cytoplasmic components are cleared in a bulk manner during nutrient deprivation (Boya et al., 2013; Kuma & Mizushima, 2010). However, in the past 10 to 15 years, numerous types of selective autophagy have been discovered (Kirkin & Rogov, 2019). In this process, autophagy can selectively recognize specific proteins, organelles, or aggregates (autophagic substrates) to promote their turnover.

Autophagy initiation was first characterized in yeast, where the growing structure initiates at the preautophagosomal structure (PAS). In mammals, the initiation of the autophagsomes occurs at a subdomain of the ER, that is characterized by enrichment of phosphatidylinositol 3-phosphoate (PI(3)P). This subdomain is called the omegasome. What determines size and shape is still not clear but evidence suggest that the actin cytoskeleton is involved in determining size and shape. In selective autophagy, the cargo itself will outline its need for size and shape of the growing phagophore (Hurley & Young, 2017).

In starvation induced autophagy, multiple stress signals converge at mTORC1 (this will also be discussed in a later section) which result in the mTORC1 phosphorylating Atg1/ULK complex to block autophagy but signals attenuating mTORC1 activity will promote and initiate autophagosome biogenesis.

Initiation begins with the Atg1/ULK complex is an initiator complex that serves as a scaffold to recruit downstream factors. Atg1/ULK complex regulates downstream factors via phosphorylation. To drive autophagosome biogenesis Atg1/ULK complex phosphorylates ATG4B, ATG9, ATG14L, BECN1, AMBRA1 and SEC23B. In selective autophagy, autophagic cargo will emit signals to stimulate autophagosome biogenesis by mediating the assembly of Atg1/ULK complex on the cargo itself by interacting with

FIP200. But the assembly of Atg1/ULK complex is common in both types of autophagy (Nakatogawa, 2020).

Formation of multiple ULK complexes are formed at the ER subdomain. ATG9-containing vesicles localize to this site, independent to ULK complex. ULK complex associates with ATG9-containing vesicles in a PI3K complex I-dependent manner. ATG9-containing vesicles is a site for PI(3)P generation that then recruits ATG16L and ATG2-WIPI complexes (Nakatogawa, 2020). Phosphatidylethanolamine (PE) lipidation of Atg8-family proteins, LC3 and GABARAPs, into the growing membrane proceed. Fusion of ATG9 vesicles generate autophagosome precursor followed by autophagosome expansion surrounding unwanted cellular content (Nakatogawa, 2020).

In selective autophagy, recognition of autophagic substrates relies on an adaptor-receptor system (Lamark & Johansen, 2021; Vargas et al., 2023). The adaptors, belonging to the ubiquitin-like ATG8-family proteins: MAP1LC3A/B/C, GABARAP and GABRAPBL1/2, are embedded into the autophagosomal membrane. PE-conjugated ATG8s recruit proteins containing one or more conserved linear motifs known as LC3-interacting regions (LIRs), with a core sequence of $[W/F/Y]_0$-X_1-X_2-$[L/V/I]_3$ (Lamark & Johansen, 2021). Selective autophagy also requires the use of selective autophagy receptors (SAR). SARs recognize the cargo, attach to the growing autophagosome and then degraded. But the role in SAR regulation of autophagy will be discussed further in a later section.

Phagosome

● LC3/GABARAP

╲ LC3-interacting region (LiR) Motif
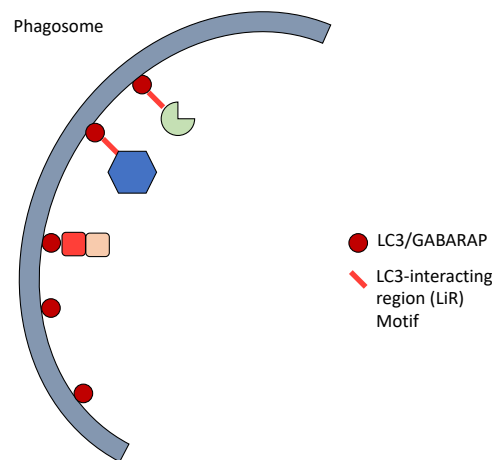
SARs physically interact with ATG8 proteins, but they also must be physically attached to a cargo. A classic example is a ubiquitin (Ub) receptor, p62/SQSTM1, which binds to ubiquitinated substrates via is Ub-associated (UBA) domain, recruiting Ub-conjugated substrates to the autophagosome (Pohl & Dikic, 2019).

There have been recent efforts in systematically trying to identify new autophagic receptors and as a result, other types of selective autophagy (Chino et al., 2019; Mancias et al., 2014; Zellner et al., 2021). It is important to note that selective autophagy is thought to be starvation independent. Which is why it becomes crucial to understanding how various autophagic receptors and cargo promote the formation of the autophagosome. In the next section I will discuss in more detail how SARs regulate autophagy in a starvation independent manner.

1.3 Regulation of Autophagy

1.3.1 mTORC1 regulation of Autophagy

As mentioned previously, there is a careful coordination between catabolic and anabolic cellular programs, where mTORC1 becomes central to the coordination. Here I will discuss the two-way coordination between mTORC1 and autophagy. To maintain homeostasis, cells integrate information about their energy and nutrient status through an elaborate array of signaling pathways. In mammals, metabolism of glucose, lipid, and protein is governed by a hormone called insulin. In the fed state, insulin suppresses autophagy by activating class I phosphatidylinositol 3-kinase (PI3-kinase) and Akt/protein kinase B, leading the eventual activation of mammalian target of rapamycin (mTOR) kinase, one of the primary negative regulators of autophagy, through direct phosphorylation of ULK1 complex (Kuma & Mizushima, 2010; Neufeld, 2010). Under a nutrient-rich state, inhibitors of mTORC1, like Rapamycin or Torin1, can activate autophagy.

As previously mentioned, mTORC1 is a primary negative regulator of autophagy, thus upstream nutrient activators of mTORC1 will in turn shut off autophagy. An example being amino acids being sensed through Rag (Ras-related GTPase) proteins activate mTOR and therefore shut-off autophagic processes (Sancak et al., 2008). Under nutrient starvation the two-way feedback between mTORC1 and autophagy is well-defined but how mTORC1 is regulating selective autophagy is less well-understood, given that selective autophagy is activated via multiple specific stimuli (Mancias & Kimmelman, 2016).

1.3.2 PKA Regulation of Autophagy

Autophagy is also regulated by Protein Kinase A. There are conflicting stances on whether PKA activates or inhibits autophagy. In yeast phosphoproteomic studies reveal PKA as phosphorylating many autophagic regulators and effectors which include the Atg1 initiation complex (Budovskaya et al., 2005; Stephan et al., 2009). Specifically in yeast, under nutrient-rich state, high levels of PKA activity inhibited autophagy by phosphorylating Atg13, preventing its association with the pre-autophagosomal structure (PAS) (Stephan et al., 2009). In human cells, phosphoproteomic studies showed similar phosphorylation patterns including the ATG8 and ATG12 conjugation systems (Filteau et al., 2015a; Isobe et al., 2017). Additionally, direct phosphorylation of LC3B by PKA was show reduced recruitment to autophagosomes (Cherra et al., 2010). However, it seems likely that the inhibitory effects on autophagy are due to RII (Grisan et al., 2021).

Like the mTORC1, autophagy also regulates PKA itself. Functional genomic screens in yeast identified genes involved in each step of autophagy, from induction to vesicle breakdown as candidate negative regulators of PKA signaling (Filteau et al., 2015a). Recently, proteomic studies have identified the capture and degradation of PKA RIα in cells (Chino et al., 2019; Zellner et al., 2021) and in neurons (Hoyer et al., 2024). Two reports characterized this degradation both in cells (Deng et al., 2021) and neurons (Overhoff et al., 2022; X. Zhou et al., 2024). In these reports, they suggest that the degradation of PKA RIα as a mechanism to increase the ratio of free PKA Cα and enhance PKA signaling. It is interesting to think that the two isoforms of PKA are regulating autophagy in different ways: Type I is being regulated by autophagy whereas type 2 is regulating autophagy (both directly and indirectly). But the two-way regulation between autophagy and PKA is complex and still remains poorly understood.

1.3.3 Activation of autophagy induced by autophagic receptors

As mentioned previously, autophagy is regulated by signaling cascades like mTORC1 and PKA, in response to external stimuli. However, selective autophagy can be initiated by the action of cargo receptors (Adriaenssens et al., 2022). The autophagic machinery can be directed to the specific cargo and mediate autophagosome biogenesis (Goodall et al., 2022; Turco et al., 2020; Zaffagnini & Martens, 2016). The recruitment of autophagic machinery to the cargo is often mediated through the interaction between the cargo receptors and FIP200 scaffold protein. Cargo receptors, like Tax1 Binding protein 1 (TAX1BP1) contain a FIP200-interacting region (FIR) which

allows them to directly interact with FIP200 and induce autophagosome biogenesis directly at the cargo meant for degradation (Turco et al., 2019; Z. Zhou et al., 2021).

Another mechanism by which receptors recruit autophagic machinery is through their ability to enrich cargo. SQSTM1/p62, as mentioned previously, recognizes ubiquitinated cargo. It is the ubiquitinated chains that act as the signal to attach to these cargo. Through its ability to oligomerize, forming homopolymers via its amino-terminal Phox and Bem1 (PB1) domain, p62 can sequester and enrich cargo protein into much larger condensates that will be recognized by selective autophagy and degraded (Ciuffa et al., 2015; Lamark et al., 2003; Pohl & Dikic, 2019). However, in the case of aggrephagy, p62 works together with NBR1 to recognize the cargo and condense the ubiquitinated proteins. NBR1(neighbor of BRCA1) then promotes the recruitment of TAX1BP1 to the condensates driving the interaction with FIP200 (Ohnstad et al., 2020; Sarraf et al., 2020; Turco et al., 2021). It is this cargo-induced activation of autophagy that enables cells to continue to degrade unwanted material while there is still mTOR activity (Adriaenssens et al., 2022; Vargas et al., 2019). But this relationship remains to be defined.

Discussion

Given the two-way feedback regulation between mTORC1 and autophagy, could there also be a way in which autophagy also feeds back on PKA signaling? Recent studies would suggest that autophagy does regulate PKA itself. Investigators identified AKAP11 as an autophagy receptor for RIa subunit (Deng et al., 2021). Additionally, other groups had similar findings in neuronal contexts but with conflicting conclusions. One group showed that the degradation of RIa was independent of AKAP11, while another study showed that RIa degradation in neurons is AKAP11 dependent (X. Zhou et al., 2024). They propose a model in which AKAP11 selectively binds RIa, upon cAMP activation, to be degraded via autophagy as a means to free up Ca and boost PKA signaling. However, during local activation of PKA, not all of RIa separates from Ca (Smith et al., 2017), making it unlikely that the entire population of Ca-associated to AKAP11 would be spared from degradation. In our study, we identified Ca as an autophagic substrate, requiring AKAP11 and RIa for degradation (see chapter 2). It is important to note that these results were obtained under steady-state conditions, which is most likely a PKA active state. Therefore, AKAP11 is mediating the degradation of the entire holoenzyme. In our phosphoproteomic data, we found that AKAP11 is mediating both PKA-dependent and independent pathways. But it still remains unknown, how on a larger scale, the AKAP11-dependent degradation of PKA helps maintain cellular homeostasis.

Through exome sequencing, AKAP11 was recently conferred a risk gene that is shared among schizophrenia (SCZ) and bipolar disorder (BP). Exome sequencing showed that AKAP11 is part of a group of rare, loss-of-function variants in SCZ. (D. Liu et al., 2023; Palmer et al., 2022; Singh et al., 2022; Sun et al., 2022).

SCZ is characterized by the Diagnostic and Statistical Manual of Mental Disorder (DSM-5) as a chronic mental illness with positive symptoms that include: delusions, hallucinations, disorganized speech and behavior, negative symptoms and cognitive impairment (Rahman & Lauriello, 2016). BP is a chronic mood disorder that causes intense shift in mood, energy levels, thinking patterns and behavior. Although having distinct diagnostic categories, genetic susceptibility for BD from common SNPs have shown to have a strong overlap with SCZ (Palmer et al., 2022). This reflects the strong influence of genetics in psychosis and mood disturbance disorders. The molecular implication of the identified risk genes is yet to be investigated. Efforts to understanding how AKAP11 may play a role into the disease pathology are currently being investigated. In akap11-mutant mice, electroencephalogram (EGG) recordings showed abnormal brain activity that overlaps with human schizophrenic patients, reflecting a systems-level role for AKAP11 in maintaining homeostasis (Herzog et al., 2023). However, understanding the mechanism in which AKAP11 carries out this role is crucial. A deep proteomic study, in which, synapses isolated from SCZ and BP found that there were significant alterations in vesicle transport/intracellular trafficking pathways. Furthermore, they found the same pathway alterations in akap11 KO and akap11 Heterozygous mice (Aryal et al., 2023). Additionally, they also found that autophagy was upregulated in these diseased states. This study provides the motivation to further characterize how AKAP11-dependent degradation of PKA may contribute to SCZ and BP pathophysiology. Furthermore, understanding how PKA and PKA signaling is modulated in these SCZ and BP patients who have the rare, protein truncating variant of AKAP11, presuming it cannot be degraded via AKAP11.

In our study, we identified an AKAP11-dependent phosphorylation site on RIa (ser83) (see chapter 2). Ser83 was further phosphorylated in the context of mutated AKAP11 LIR compared to the wild-type rescue, suggesting that AKAP11 autophagic degradation is mediating RIa degradation but also shaping cellular signaling. Interestingly, this phosphosite was hyperphosphorylated in autophagy incompetent cells (X. Zhou et al., 2024), further supporting our model where the growing autophagosome provides a signaling scaffold for AKAP11-bound PKA, while also mediating its degradation. It is yet to be determined which kinase phosphorylates this specific site and the kinase relationship with AKAP11. Additionally, it needs to be determined the downstream effects of this phospho-site and the importance of this phosphorylation in the context of SCZ and BP. Our study provides a blueprint for future studies that can be performed in a more disease relevant model.

CHAPTER 2 AKAP11 coordinates an autophagy-dependent regulatory checkpoint that shapes neuronal PKA signaling.

Ashley Segura-Roman, Yemima R. Citron, and Roberto Zoncu conceived of and designed the study. Ashley Segura-Roman, Yemima R. Citron, Myungsun Shin, Nicole Sindoni, Alex Maya-Romero, Simon Rapp, and Claire Goul and Roberto Zoncu generated key reagents and performed all experiments. Ashley Segura-Roman, Yemima R. Citron, Myungsun Shin, Nicole Sindoni and Roberto Zoncu analyzed the data and interpreted results. Ashley Segura-Roman, Yemima R. Citron, and Roberto Zoncu wrote the manuscript.

2.1 Chapter Summary

Protein Kinase A (PKA) is regulated spatially and temporally via scaffolding of its catalytic (Ca/b) and regulatory (RI/RII) subunits by the A-kinase-anchoring proteins (AKAP). PKA engages in poorly understood interactions with autophagy, a key degradation pathway for neuronal cell homeostasis, partly via its AKAP11 scaffold. Mutations in AKAP11 drive schizophrenia and bipolar disorders (SZ-BP) through unknown mechanisms. Through proteomic-based analysis of immunopurified lysosomes, we identify the Ca-RIa-AKAP11 holocomplex as an autophagy-regulated signaling complex. AKAP11 scaffolds Ca- RIa to the autophagic machinery via its LC3-interacting region (LIR), enabling both PKA regulation by upstream signals, and its autophagy-dependent degradation . We identify Ser83 on the RIa linker-hinge region as an AKAP11-dependent phospho-residue that modulates RIa-Ca binding and cAMP-induced PKA activation. Mutating AKAP11-LIR alters Ser83 phosphorylation, supporting an autophagy-dependent checkpoint for PKA signaling. Accordingly, ablating AKAP11 in induced pluripotent stem cell-derived neurons reveals dysregulation of multiple PKA-dependent and independent pathways. Thus, AKAP11 shapes multiple PKA-dependent signaling events, providing a possible mechanistic link to SZ/BP pathogenesis.

2.2 Introduction

Maintenance of cellular homeostasis relies on precise regulation of master regulatory kinases such as Protein Kinase A (PKA), mechanistic Target of Rapamycin Complex 1 (mTORC1) and AMP-regulated Protein Kinase (AMPK). These kinase hubs integrate a wide range of upstream stimuli to generate downstream responses that govern cell growth, differentiation, survival and metabolic adaptation. Moreover, their activities are fine-tuned by post-translational events such as phosphorylation and ubiquitylation, leading to their dynamic assembly, disassembly, sequestration and relocalization (X. Zhou et al., 2024).

   PKA is a prominent Ser/Thr kinase that transduces cyclic adenosine monophosphate (cAMP) -mediated signals from many different hormones and neurotransmitters to instruct biological responses ranging from regulation of glucose and lipid metabolism in peripheral tissues, to memory formation and consolidation in the brain (Kandel, 2012; London et al., 2020; Monterisi & Zaccolo, 2017; Tomek & Zaccolo, 2023). In its inactive state, PKA exists as a holoenzyme composed of a homodimer of two regulatory (R) subunits, each of which in turn holds and inhibits two catalytic subunits. Binding of cAMP to two nucleotide binding domains (NBD) on each R subunit induces a conformational change that frees up the C-subunit active site, enabling

phosphorylation of a wide variety of downstream substrates (Kim et al., 2007; Taylor et al., 2013; Wu et al., 2007).

Four subtypes of R-subunits, RIa, RIb, RIIa, and RIIb, form as many distinct homodimers; in addition to C-subunits, each R-dimer, in turn, can bind to several A-kinase anchoring proteins (AKAPs). AKAP proteins organizes PKA signaling into a distributed intracellular network, where microdomains of PKA holoenzymes, scaffolded to different subcellular compartments, perform specific regulatory actions upon local elevation of cAMP levels (Scott et al., 2013). Detailed mechanistic studies of AKAP proteins have conclusively demonstrated their ability to link PKA activity to specific organelles and cellular compartments, including the plasma membrane, nuclear envelope, mitochondria, Golgi apparatus, lipid droplets and centrosome (Monterisi & Zaccolo, 2017; Omar & Scott, 2020).

AKAP11 (also known as AKAP220) is among the least well understood AKAPs. This 220-KDa PKA-scaffolding protein has been implicated in processes such as actin turnover (Logue, Whiting, Tunquist, Langeberg, et al., 2011), microtubule dynamics (Logue, Whiting, Tunquist, Sacks, et al., 2011), and osmoregulation (Whiting et al., 2016). AKAP11 has two binding sites for the regulatory subunits, one which binds to both RIa and RIIa, whereas a second one solely binds to RIIa (Whiting et al., 2015). Along with the PKA holoenzyme, AKAP11 scaffolds glycogen synthase kinase (GSK) IIIb, possibly allowing cross-regulation between the two kinases (Tanji et al., 2002; Whiting et al., 2015). AKAP11 also binds to protein phosphatase 1 (PP1), possibly as part of an integrated system to quickly activate and then shut down downstream substrates for both PKA and GSKIII-b (Schillace & Scott, 1999).

Recently, polymorphisms in the AKAP11 gene sequence that lead to protein truncation and loss-of-function have been strongly associated with increased risk for schizophrenia (SCZ) and bipolar disorder (BP) (Herzog et al., 2023; D. Liu et al., 2023; Palmer et al., 2022). A deep-proteomic study comparing brain tissue samples from SCZ and BP patients with synaptosomal preparations from AKAP11-knockout mice revealed shared alterations in the abundance of protein classes that are important for brain function, including mitochondria, vesicle trafficking and tethering (Aryal et al., 2023). However, the molecular links between AKAP11 deficiency and neuronal dysfunction that leads to SCZ and BP remain unknown.

Several reports have implicated AKAP11 in directing PKA to specific vesicle populations. AKAP11 was shown to recruit RIa to multivesicular bodies (MVBs), but only when RIa is not bound to Ca such as in high cAMP concentrations (Day et al., 2011). More recently, AKAP11 was proposed to function as a selective autophagy receptor that, by interacting with ATG8-family proteins, causes selective RIa capture and degradation into autophagosomes, while sparing Ca from degradation (Deng et al., 2021; X. Zhou et al., 2024).

Autophagy is a vesicular catabolic pathway that singles out proteins, macromolecules and organelles for capture within double-membraned autophagosomes, which subsequently deliver their cargo to lysosomes for degradation (Yamamoto et al., 2023). Recognition of autophagic substrates relies on a receptor-adaptor system (Lamark & Johansen, 2021; Vargas et al., 2023). Autophagic adaptors of the ubiquitin-like ATG8-family: MAP1LC3A/B/C, GABARAP and GABRAPBL1/2, are inserted in the autophagosomal membrane via their C-terminal conjugation to phosphatidylethanolamine (PE). ATG8-family adaptors recognize conserved linear motifs known as LC3-interacting regions (LIRs) on selective autophagic receptors, which in turn recruit various cargo to the nascent autophagosome (Ichimura et al., 2008; Kirkin & Rogov, 2019).

Consistent with the critical roles of autophagy in nutrient homeostasis and cellular quality control, this pathway is subjected to regulation by master nutrient-sensing kinases such as mTORC1, which negatively regulates the autophagosome-nucleating ULK1 complex under high nutrients, and AMPK, which stimulates several autophagic regulatory complexes during energy shortage (Kaur & Debnath, 2015; Shin & Zoncu, 2020). Conversely, emerging evidence suggests that autophagy can exert feedback regulation on upstream signaling pathways: for example, nutrients generated by autophagic breakdown of macromolecules can reactivate mTORC1 and shut down AMPK signaling during recovery from starvation (G. Y. Liu & Sabatini, 2020; Shin & Zoncu, 2020).

The relationship between PKA signaling and autophagy is complex and not fully understood. Phosphoproteomic studies in yeast and human cells identified many autophagic regulators and effectors as PKA substrates, including the ATG1/ULK1 initiation complex, the ATG8 and ATG12 conjugation systems, as well as accessory factors and adaptors (Budovskaya et al., 2005; Grisan et al., 2021; Isobe et al., 2017; Stephan et al., 2009). PKA-dependent phosphorylation of LC3B and ATG16L1 were shown to inhibit autophagosome formation in neurons and endothelial cells, respectively, suggesting that, like mTORC1, PKA may inhibit autophagy (Cherra et al., 2010; Zhao et al., n.d.). Conversely, functional genomic screens in yeast identified genes involved in each step of autophagy, from induction to substrate breakdown, as candidate negative regulators of PKA signaling (Filteau et al., 2015b).

The findings that AKAP11 promotes autophagic degradation of RIa has led to a model in which selective RIa elimination increases the ratio of free C-subunit, thereby promoting PKA signaling (Deng et al., 2021; X. Zhou et al., 2024). This mechanism was proposed to potentiate C-mediated phosphorylation of PKA-cAMP response element-binding (CREB) transcription factor, boosting mitochondrial metabolism and conferring resistance to glucose deprivation (Deng et al., 2021). Along similar lines, a further study

proposed that autophagy-dependent elimination of RIb in neurons frees up Ca to enhance PKA signaling at the synapse (Overhoff et al., 2022).

However, these models need to be evaluated in light of well-established features of PKA regulation. First, the R-subunit does not play a purely inhibitory role toward the C-subunit. On the contrary, by scaffolding C to different AKAP proteins, R helps place the latter in proximity to numerous organelle-specific substrates (Means et al., 2011; Monterisi & Zaccolo, 2017; Omar & Scott, 2020; Pidoux et al., 2011). Thus, decreasing the stoichiometry of R- to C-subunits would be expected to have mixed effects on downstream signaling, favoring some phosphorylation events while decreasing others. Second, recent evidence suggests that, at physiological cAMP levels found within the cell, C-subunits do not completely separate from the R-subunit-AKAP complex. Instead, the three components remain bound in an open, signaling-competent conformation that is capable of substrate recognition and phosphorylation (Smith et al., 2013, 2017). Thus, autophagic capture of AKAP11-RIa seems unlikely to completely spare C-subunits from degradation.

To achieve a fine-grained understanding of how autophagy regulates PKA, and possibly other multiprotein signaling complexes, we combined immunoisolation and proteomic-based profiling of lysosomes from autophagy competent and deficient cells with bioinformatic analysis of protein-protein interaction datasets. These experiments identify the PKA holoenzyme, primarily composed of the RIa and Ca subunits and AKAP11, as the sole kinase complex degraded by autophagy. In agreement with previous reports, AKAP11 bridges RIa to LC3B and GABARAP via its LIR motif. However, we find that Ca binds to AKAP11 via RIa and is degraded, along with RIa, in an autophagy- and AKAP11-dependent manner. Phosphoproteomic analysis in iPSC-derived neurons reveals that AKAP11 coordinates a regulatory checkpoint by enabling RIa phosphorylation by upstream kinases; accordingly, depleting AKAP11 or disabling its interaction with the autophagy machinery led to dysregulation of numerous PKA-dependent signaling programs. Collectively, our data identify AKAP11 as a central signaling hub that plays a critical role in shaping PKA-dependent signaling responses. Alteration of these signaling programs upon AKAP11 loss may contribute to the pathogenesis of SZ/BP.

Results
Proteomic and bioinformatic identification of multiprotein autophagic substrates.
To systematically identify multiprotein complexes degraded in an autophagy-dependent manner, we carried out lysosomal immunoisolation followed by proteomic-based profiling from control HEK-293T cells versus HEK-293T cells deleted for an essential autophagic regulator, the E2-like factor ATG7, both stably expressing the lysosomal affinity tag TMEM192-mRFP-[3x]HA (Abu-Remaileh et al., 2017; Davis et al.,

2021) (Fig. 1A and Fig. S1A-S1B). To unambiguously distinguish lysosomal resident
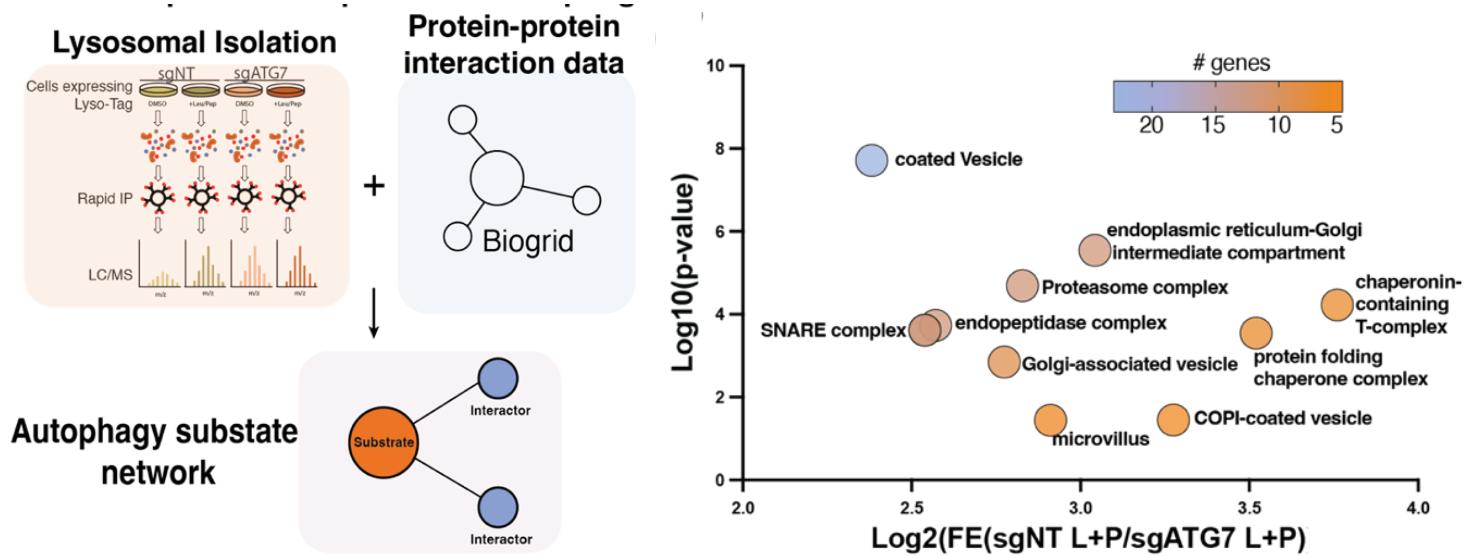
proteins from *bona fide* substrates, we
compared lysosomal immunoprecipitates from DMSO-treated control and ATG7-KO
cells, versus cells treated with the protease inhibitor cocktail, leupeptin + pepstatin
(L+P) (Davis et al., 2021). Proteins that showed selective accumulation in L+P-treated
control lysosomes included canonical autophagic receptors CALCOCO2, NBR1,
TAX1BP1 and NCOA4, along with transmembrane and extracellular proteins that reach
the lysosome via endocytic uptake and endosomal trafficking (Supplementary data 1).
As expected, autophagic receptors were depleted in lysosomes immunopurified from
ATG7-KO cells (Supplementary data 1), establishing a clear pattern for recognition of
bona fide autophagic substrates.

Gene Ontology (GO) analysis showed differential accumulation of several
classes of putative autophagic substrates in lysosomes from control, L+P treated cells
versus ATG7-KO, L+P-treated cells. The most autophagy-dependent substrate
categories included factors involved in protein folding, transport and quality control (Fig.
1B and Fig. S1C).

We next analyzed the proteomic data through a custom-written bioinformatic
pipeline that clusters proteins based on physical interaction (BioGRID database) (Fig.
1A and S1B). The resulting network view identified several multiprotein complexes as
novel substrates of autophagic degradation (Fig. 1C). We identified complexes involved
in protein quality control, including the proteasome (12 subunits detected with p-value
=2.05E-05) and the CCT/TRiC chaperone complex (7 subunits) (Fig. 1D and
Supplementary data 1). Also detected was the HSP90 chaperone complex, including
HSP90a class A and B, their p23/PTGES3 and FKBP4 cofactors, as well as HSP70,
which, while not stably bound to HSP90, functions in close association with HSP90 on
substrate proteins(Moll et al., 2022) (Fig. 1D and Supplementary data 1). The

enrichment of protein quality control factors may reflect their autophagy-dependent degradation, along with protein clients due to folding stress or nutrient depletion. Notably, the CCT/TRiC component CCT2, which scored in our analysis, was recently proposed to function as an aggrephagy receptor (Ma et al., 2022).

Our pipeline also identified multiprotein complexes involved in signal transduction, specifically the catalytic and one regulatory subunits of protein phosphatase 2 (PPP2CA and PPP2R1A, respectively), and the PKA enzyme complex composed of the Ca catalytic subunit, the RIa and RIIa regulatory subunits, and the AKAP11 (also known as AKAP220) scaffolding protein (Fig. 1D and Supplementary data 1).
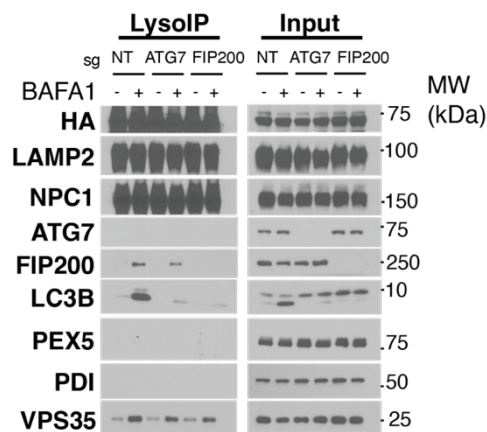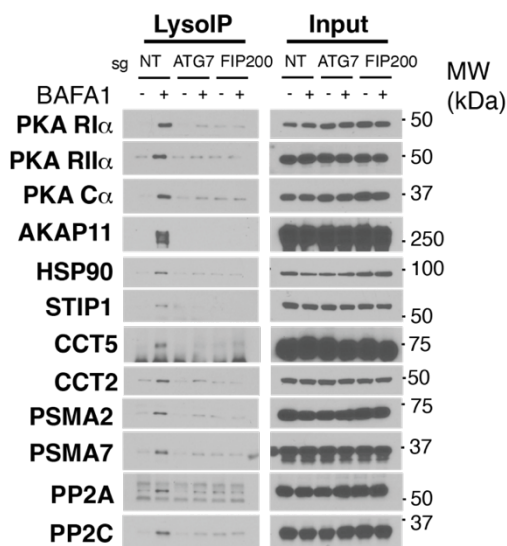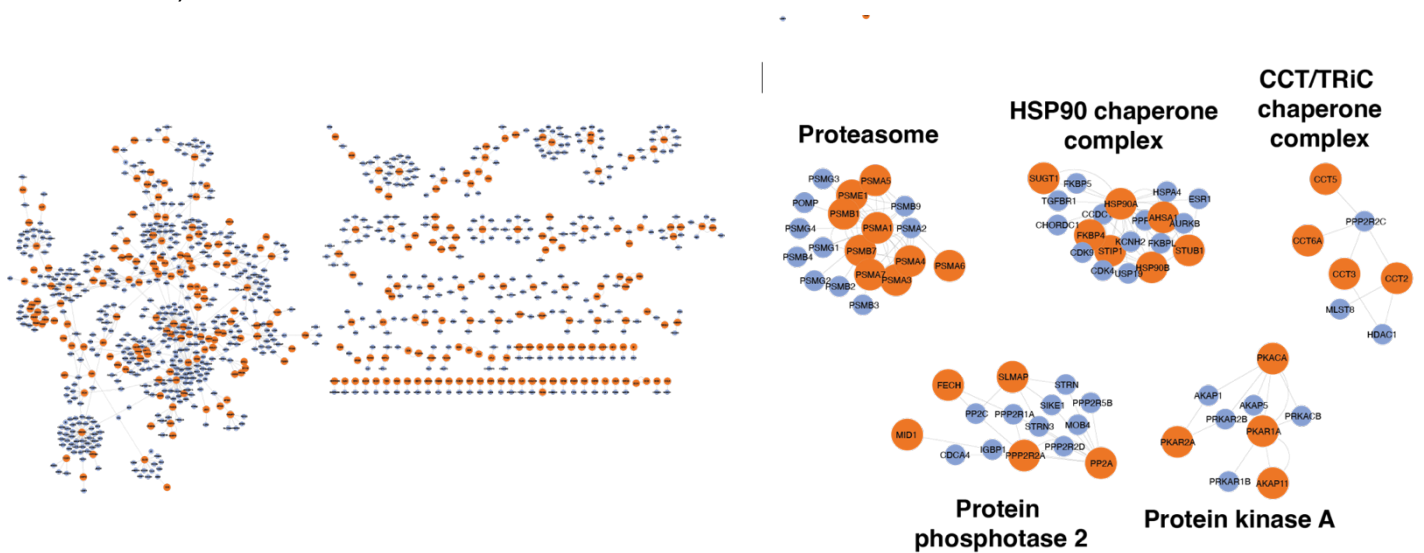
The PKA holoenzyme is a substrate for autophagic degradation

To independently validate the proteomic data, we immunoisolated lysosomal samples from control and ATG7-KO HEK-293T cells, as well as from cells deleted for FIP200, a component of the ULK1 complex that is essential for autophagy initiation (Yamamoto et al., 2023). We carried out lyso-IP both in baseline conditions and following treatment with the vacuolar H^+ATPase (v-ATPase) inhibitor, Bafilomycin A1 (BafA1), which, like L+P, inhibits substrate breakdown within the lysosomal lumen (Fig. 1E). Immunoblotting of these samples confirmed the autophagy-dependent degradation of the multiprotein complex components detected by mass spectrometry, including the proteasome, HSP90, CCT/TriC, PP2A (Fig. 1E). Supporting autophagic degradation of the PKA holoenzyme, RIa, RIIa, Ca and AKAP11 were clearly detected in lysosomes from control cells treated with BafA1, but not in lysosomes from BafA1-treated ATG7- and FIP200-KO cells (Fig. 1E). In light of recently proposed models of autophagy-dependent activation of PKA (Deng et al., 2021; Overhoff et al., 2022; X. Zhou et al., 2024), and the recently discovered association of AKAP11 mutations with SCZ and BP (Herzog et al., 2023; D. Liu et al., 2023; Palmer et al., 2022), we decided to further investigate the Ca-R1a-AKAP11 complex as a potential autophagy substrate.

To gain a quantitative understanding of PKA-AKAP11 complex degradation, we visualized the lysosomal mass spectrometry data (Supplementary data 1) as volcano plots of Log2 fold change over -Log10 p-value. These plots showed that RIa is among the autophagic substrates most enriched by L+P treatment, on par with canonical autophagic receptors such as TAX1BP1 and p62, whereas Ca and AKAP11 were stabilized to a lesser degree (Fig. 2A). The same relative enrichment was found when comparing lysosomes from L+P-treated wild-type versus ATG7-deleted cells (Fig. 2B).

Autophagy-dependent capture of the PKA holoenzyme was also evident in immunofluorescence-based experiments. In cells stably expressing FLAG-tagged RIa, blocking lysosomal proteolysis with BafA1 led to pronounced accumulation of FLAG-R1a in LAMP2-positive lysosomes of control, but not ATG7-deleted, HEK-293T cells (Fig. 2C and 2D). Similarly, in HEK-293T cells in which endogenous Ca is C-terminally tagged with mNeon (Cho et al., 2022), treatment with BafA1 led to pronounced accumulation of Ca-mNeon in LAMP2-positive lysosomes that was abolished by shRNA-mediated knock down of FIP200, consistent with autophagy-dependent capture and degradation of Ca (Fig. 2E and 2F and Fig. S1D).

In conclusion, converging evidence from organelle proteomics and immunolocalization support concomitant lysosomal degradation of both regulatory and catalytic PKA subunits via an autophagy-dependent mechanism.

AKAP11 mediates capture of the PKA holoenzyme

It was previously reported that AKAP11 promotes autophagic degradation of a fraction of the RIa pool (Deng et al., 2021; X. Zhou et al., 2024). However, our detection of Ca in immunopurified lysosomes, as well as by colocalization analysis in intact cells, indicate that autophagy mediates degradation of not just R1a, but of the entire PKA holoenzyme (Fig. 1D-1E, 2E-2F). To test whether autophagic Ca degradation is also AKAP11-dependent, we stably expressed the lysosomal affinity tag in both control and AKAP11-deleted HEK-293T cells, and immunoblotted lysosomal samples for multiple PKA proteins. This analysis clearly showed that both Ca and RIa were strongly depleted from lysosomes immunopurified from AKAP11-KO cells (Fig. 3A).
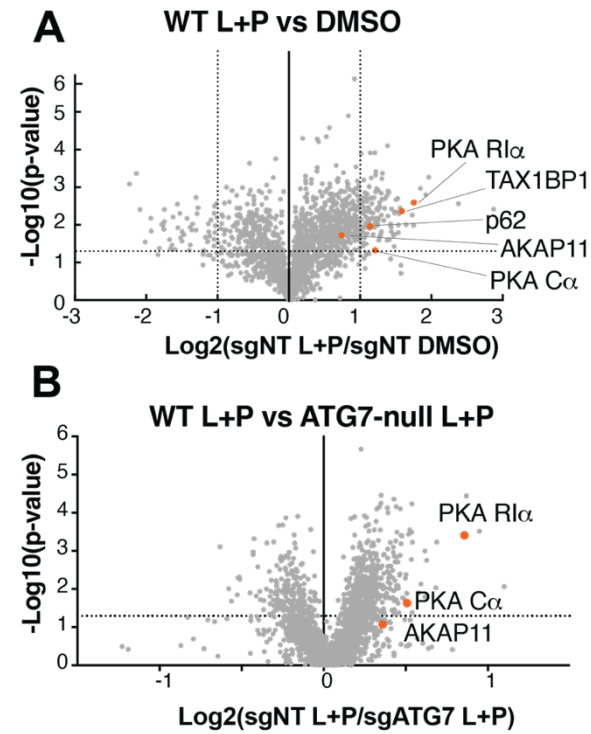
Whereas the R-AKAP interaction is relatively stable (in the nanomolar range), Ca progressively dissociates from the R-AKAP complexes as cytoplasmic concentrations of cAMP increase(Bock et al., 2024). However, recent structural and biochemical evidence indicates that
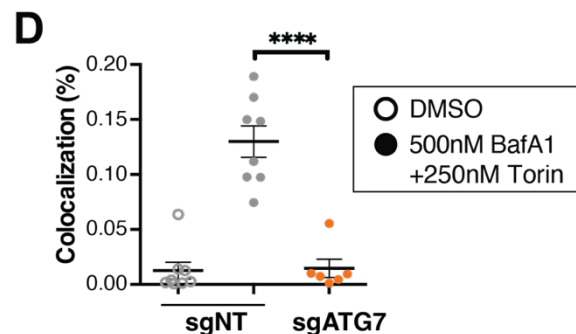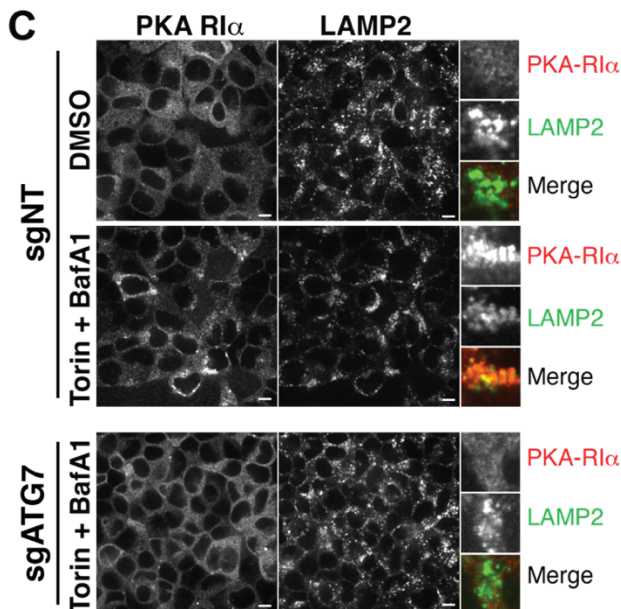
concentrations of cAMP that are sufficient to activate PKA signaling do not cause complete Ca dissociation from the R-AKAP complex. Instead, the AKAP-holoenzyme remains associated while adopting a range of dynamic conformations that are compatible with substrate engagement and phosphorylation (Smith et al., 2013, 2017). In line with this idea, HA-tagged AKAP11 co-immunoprecipitated both RIa and Ca at the steady-state levels of cAMP that exist under full media conditions. To achieve complete separation of Ca from the R1a-AKAP11 complex, we had to treat cells with the adenylyl cyclase activator, forskolin, at >1mM concentrations, which lead to supra-physiological cAMP levels in the cell(Smith et al., 2017) (Fig. 3B).
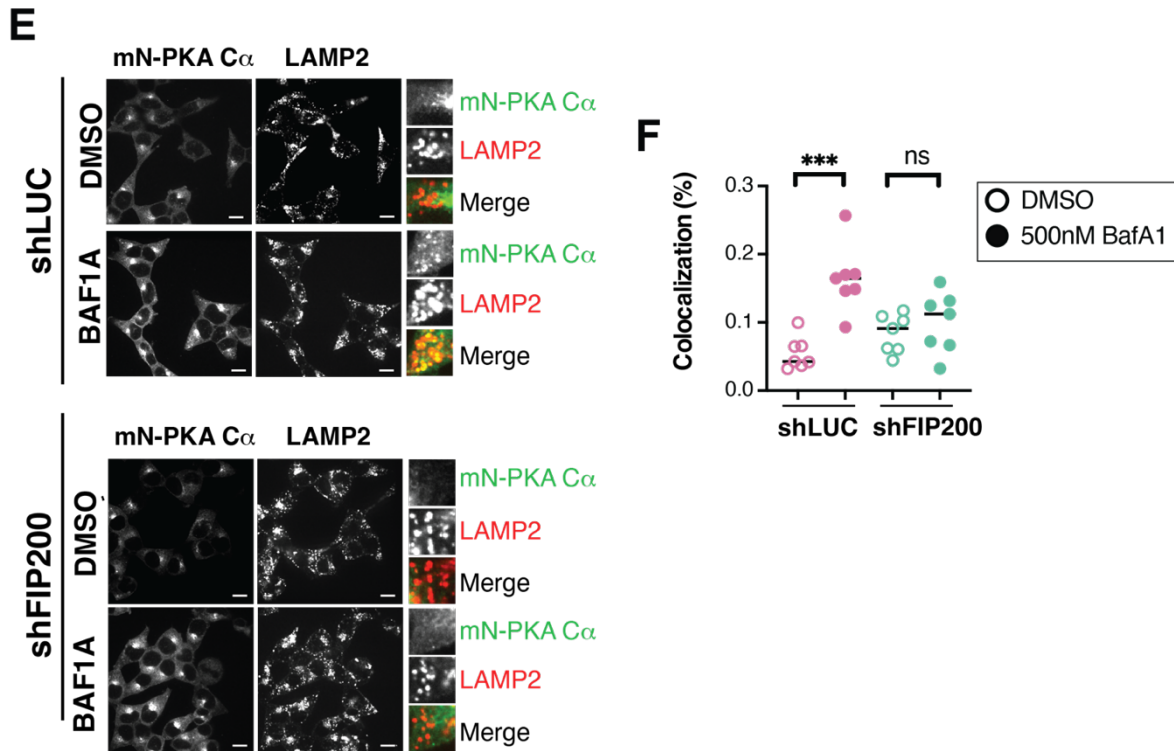
To be captured into autophagosomes, substrate proteins must interact with Atg8-family proteins LC3A/B/C or GABARAP, either via an LC3-interacting region (LIR) within their amino acid sequence, or indirectly through a selective autophagic receptor (Adriaenssens et al., 2022; Kirkin & Rogov, 2019). In co-immunoprecipitation (co-IP) experiments, GFP-tagged LC3B and GABARAP bound to R1a, Ca and AKAP11 with relatively high strength (Fig. 3C). These interactions were largely abolished when using point mutants in the hydrophobic groove of LC3 and GABARAP that impair recognition of canonical LIR motifs (P52A and Y46A, respectively) (Ichimura et al., 2008; Kirkin & Rogov, 2019) (Fig. 3C, top). Supporting the requirement for AKAP11 in autophagic capture of the PKA holoenzyme, GFP-LC3B and GFP-GABARAP failed to immunoprecipitated endogenous RIa and Ca when expressed in AKAP11-deleted cells,

whereas their binding to p62/SQSTM1 was unaffected by lack of AKAP11 protein (Fig. 3C, bottom).

Similar to HA-AKAP11, GFP-LC3B co-immunoprecipitated both RIa and Ca in full media conditions. Stimulating GFP-LC3B-expressing cells with increasing concentrations of forskolin progressively reduced the amount of Ca immunoprecipitated by GFP-LC3B, consistent with Ca interacting with LC3B indirectly, via its association with R1a (Fig. 3D). However, as for the AKAP11 co-IP experiments (Fig. 3B), Ca fully separated from LC3B only at supraphysiological concentrations of forskolin (>1mM) (Fig. 3D).

Thus, under steady-state conditions autophagy captures and degrades the
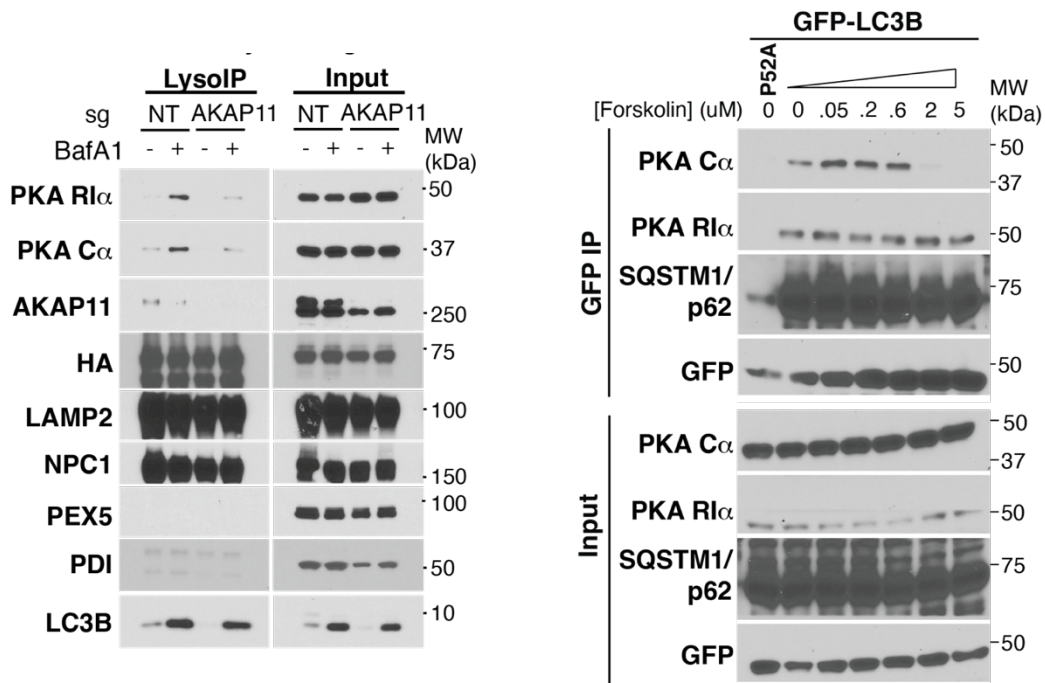
AKAP11-bound pool of PKA holoenzyme via association of both RIa and Ca with AKAP11 and LC3/GABARAP.
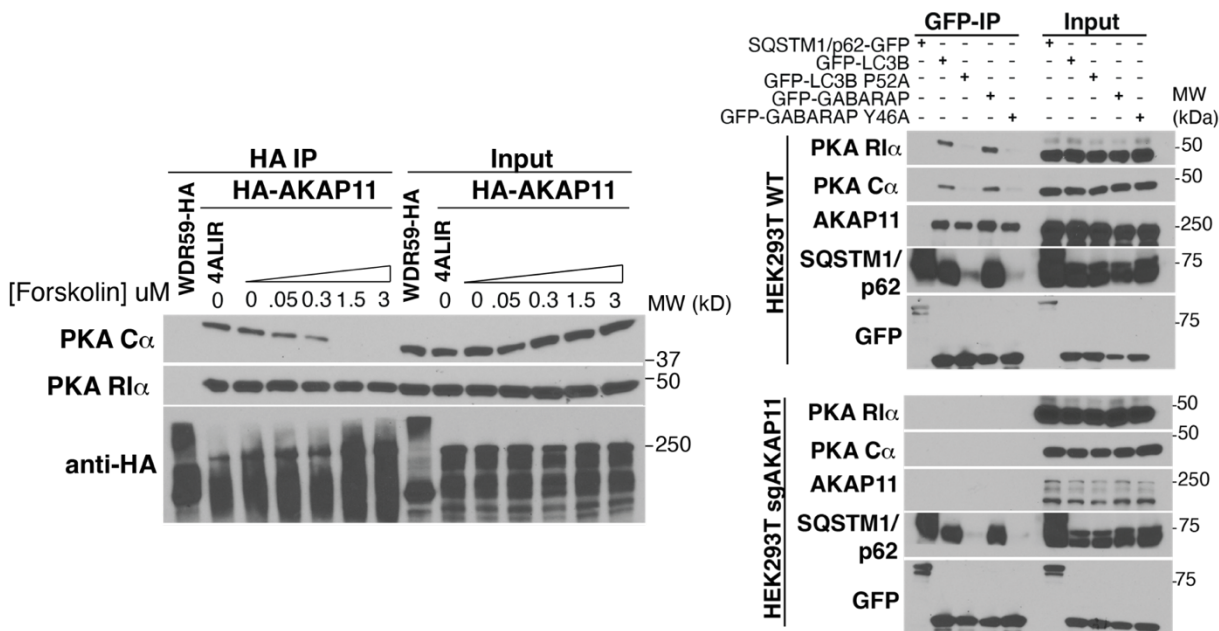
AKAP11 binding to LC3 and R1a is required for autophagic degradation of the PKA holoenzyme.

We next tested the mechanisms underlying autophagic capture of the AKAP11-containing PKA holoenzyme. Human AKAP11 contains a putative LIR motif, WSNL, at a.a. 1736-1739 (Deng et al., 2021). Whereas wild-type, V5-tagged AKAP11 (stably expressed in AKAP11-deleted HEK-293T cells) was readily detected within LAMP2-positive lysosomes upon BafA1-treatment, mutating the WSNL motif to four alanines caused the resulting AKAP11[4ALIR] mutant to be largely excluded from lysosomes and instead maintain a diffuse staining pattern upon BafA1 treatment (Fig. 4A-4B).

As the 1736-1739 LIR motif of AKAP11 was shown to be required for AKAP11-mediated R1a degradation (Deng et al., 2021), we sought to determine its requirement

Fig.4: the AKAP11 LIR motif mediates autophagic capture of the PKA holoenzyme

A V5-AKAP11 LAMP2

B

C mN-PKA Cα LAMP2

D
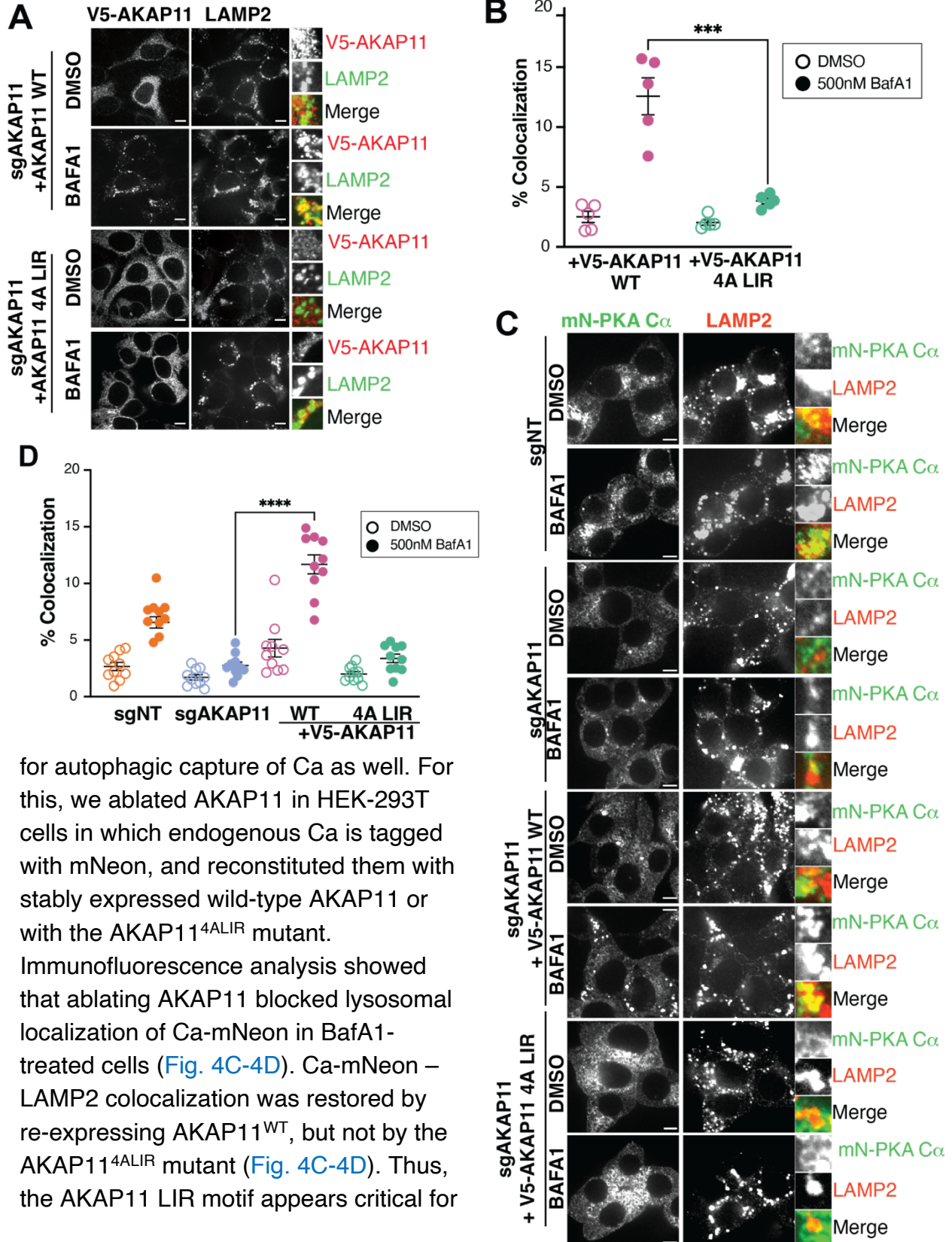
for autophagic capture of Ca as well. For this, we ablated AKAP11 in HEK-293T cells in which endogenous Ca is tagged with mNeon, and reconstituted them with stably expressed wild-type AKAP11 or with the AKAP11[4ALIR] mutant. Immunofluorescence analysis showed that ablating AKAP11 blocked lysosomal localization of Ca-mNeon in BafA1-treated cells (Fig. 4C-4D). Ca-mNeon – LAMP2 colocalization was restored by re-expressing AKAP11[WT], but not by the AKAP11[4ALIR] mutant (Fig. 4C-4D). Thus, the AKAP11 LIR motif appears critical for

autophagic capture of the PKA holoenzyme.

Because RIa bridges AKAP11 with Ca (Fig. 3B), we also examined potential roles for RIa in promoting autophagic degradation of the holoenzyme. We generated RIa-deleted HEK-293T cells via CRISPR-Cas9,and carried out lyso-IP from these cells. As expected, deleting RIa prevented capture of Ca in lysosomes (Fig. 4E). Interestingly, the levels of lysosomal AKAP11 were also suppressed in lysosomes from RIa-deleted cells, suggesting that AKAP11 must be bound to RIa in order for its capture by the autophagic machinery to occur (Fig. 4E)
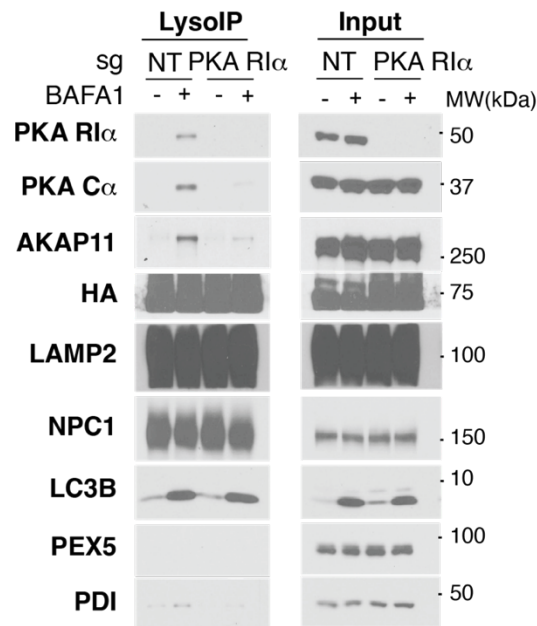
Phosphoproteomic analysis in iNeurons reveals AKAP11-dependent PKA regulation.

Our finding that AKAP11 binds to and degrades the entire PKA holoenzyme prompted us to dissect its regulatory roles toward PKA signaling. Because AKAP11 is highly expressed in the brain, and given the strong association between AKAP11 gene truncations and SZ/BP (Herzog et al., 2023; D. Liu et al., 2023; Palmer et al., 2022), we carried out these experiments in induced pluripotent stem cell (iPSC)-derived neurons. Using CRISPR-interference (CRISPRi), we first suppressed AKAP11 expression in iPSCs that can be differentiated into inducible cortical neurons (i3 neurons) via doxycycline-driven expression of neurogenin-2 (NGN2)(Fernandopulle et al., 2018) . Both prior to differentiation and at 7 days post-NGN2 induction, we verified efficient silencing of AKAP11 by three independent single-guide RNAs (sgRNAs). Consistent with the results in HEK-293T cells, all AKAP11-targeting sgRNAs led to strong

stabilization of RIa and, to a lesser extent, of Ca (Fig. 5A, and Fig. S2A-S2D). AKAP11-depleted i3 neurons were morphologically similar to control neurons (Fig. 5B).

Fig.5: AKAP11 mediates PKA-dependent and independent signaling in i3 Neurons
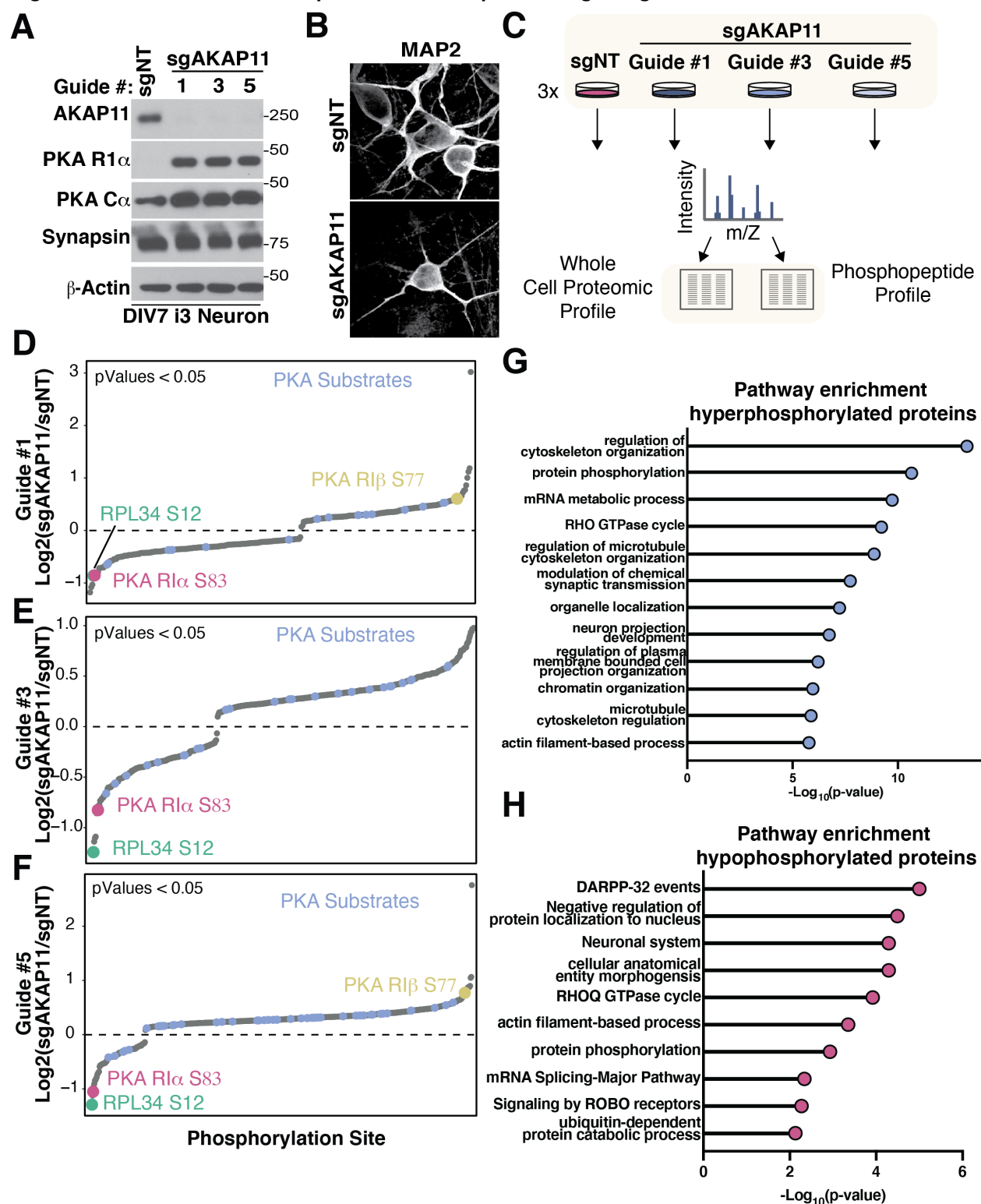
We employed phosphoproteomic analysis to determine the effect of AKAP11 loss on PKA-dependent signaling in i3 neurons (Fig. 5C). Because RIa and Ca stabilization was clearly detectable under standard growth conditions (Fig. 5A and S2B-S2D), we carried out our analysis without further stimulating PKA activity or autophagy. We detected 228 peptides, belonging to 174 proteins, phosphorylation of which was significantly (p<0.05) altered in at least 2 out of 3 sgAKAP11 i3neuron lines (Fig. 5D-5F and supplementary data 2: phospho-peptide signals normalized by total protein levels). Notably, only 5.7% (13 sites) of differentially phosphorylated peptides matched the consensus PKA target site, whereas 94.3% were not predicted to be PKA sites (supplementary data 2).

Pathway enrichment analysis of differentially phosphorylated proteins revealed that, in line with its reported functions in non-neuronal lines8/9/24 11:52:00 AM AKAP11 controls phosphorylation of proteins involved in microtubule polymerization/depolymerization and regulation of the actin cytoskeleton (Logue, Whiting, Tunquist, Langeberg, et al., 2011; Logue, Whiting, Tunquist, Sacks, et al., 2011; Whiting et al., 2016) (Fig. 5G-5H and supplementary data 2). Other differentially phosphorylated categories included synaptic function, neuronal morphogenesis and signaling (Fig. 5G-5H and supplementary data 2).

Of the 13 *bona fide* PKA target sites differentially regulated in an AKAP11-dependent manner, 7 sites were hypophosphorylated in AKAP11-depleted neurons, whereas 6 sites were hyperphosphorylated. A notable site was Ser12 on the large ribosomal protein 34 (RPL34), which was among the most hypophosphorylated sites in all three AKAP11-depleted lines (Fig. 5D-5F and supplementary data 2). Ser12 is highly conserved, and is located in the extended N-terminal region of RPL34, and lies in close proximity to several ribosomal RNA (rRNA) molecules within the large subunit core(Anger et al., 2013) (Figure S3A-S3B). The position of Ser12 deep within the large ribosomal subunit core predicts that its PKA- and AKAP11-dependent phosphorylation could significantly impact ribosomal large subunit assembly and stability. According to published phosphoproteomic datasets (www.phosphosite.org), Ser12 is the most commonly detected phospho-site on RPL34, supporting its role as a putative regulatory site for the ribosome.

Among the most hypo-phosphorylated non-PKA substrate peptides in all three AKAP11-deleted i3 neuron lines was Ser83 in the RIa subunit (Fig. 5D-5F and supplementary data 2). Ser83 is highly conserved, is located within the linker–hinge region of R1a, N-terminally proximal to the inhibitory sequence (IS) (Figure S3C-S3D), and phosphorylation of several residues in this region had previously been proposed to regulate the stability of IS binding to the catalytic cleft of Ca and, thus, the efficiency of Ca inhibition(Han et al., 2013; Haushalter et al., 2018). Ser83 is a commonly detected phospho-site on RIa (www.phosphosite.org), thus it is likely to represent a *bona fide*

regulatory site that, upon phosphorylation by upstream kinases (see Discussion) may fine-tune the activity levels of AKAP11-bound PKA.

Finally, in addition to RIa, its brain-specific paralog RIb, and Ca levels, proteomic analysis revealed significant changes in the total levels of numerous other proteins (Fig. S2B-S2D and supplementary data 2). Protein classes that were especially increased in AKAP11-depleted i3 neurons included ribosome biogenesis and rRNA processing factors, an effect possibly linked to our finding of AKAP11- and PKA-dependent RPL34 phosphorylation on Ser12.

In summary, our phosphoproteomic analysis in i3 Neurons reveals a complex network downstream of AKAP11, whereby both PKA-dependent and PKA-independent phosphorylation events are either promoted or antagonized in an AKAP11-dependent manner.

AKAP11-dependent RIa phosphorylation at Ser83 modulates PKA activation.

We next sought to mechanistically dissect the role of AKAP11 and its interaction with the autophagy machinery in regulating the phosphorylation events that we identified in i3 neurons. To this aim, we carried out parallel whole-cell phosphoproteomic analysis in control, AKAP11-deleted and AKAP11-deleted cells reconstituted with exogenous wild-type AKAP11 or with the AKAP11[4ALIR] mutant (Fig. 6A). We employed HEK-293T cells for these experiments as they were more amenable than the i3 neuron system to deletion-reconstitution protocols. As expected, re-expressing (V5-tagged) wild-type AKAP11 in sgAKAP11 cells decreased the elevated endogenous RIa levels, whereas V5-AKAP11[4ALIR] failed to bring RIa down to wild-type levels, albeit not completely (Fig. S4A).

By comparative phosphoproteomic analysis of the AKAP11-deleted and reconstituted samples (carried out, as in i3 neurons, under standard growth conditions), we detected 81 phosphorylated peptides that changed significantly as a function of AKAP11 status upon normalization by total levels of their respective proteins (supplementary data 3). We focused on phospho-peptides that, if increased by deletion of AKAP11, were decreased back toward control levels by re-expressing wild-type AKAP11 and, vice-versa, phospho-peptides whose abundance was decreased by AKAP11 deletion and restored by re-expressing wild-type AKAP11 (Fig. 6B-6C, supplementary data 3).

Compared to i3 neurons, fewer canonical PKA substrates were differentially phosphorylated in an AKAP11-manner in HEK-293T cells, possibly reflecting a predominant role for AKAP11 in the brain. However, in agreement with the i3 neurons one of the most hypo-phosphorylated peptides in AKAP11-deleted cells that were restored by AKAP11[WT] re-expression was Ser83 in RIa (Fig. 6B-6C). As mentioned above, the location of S83 within the hinge-loop region of RIa suggests that its

phosphorylation may regulate Ca activation. Supporting this idea, phosphorylation of nearby Ser101 by cGMP-dependent protein kinase (PKG) was shown to destabilize IS-Ca interaction, thereby contributing to PKA activation (Haushalter et al., 2018).

To dissect the role of S83 phosphorylation, we carried out a modification of previously described semi-reconstituted phosphorylation assays (Haushalter et al.,

Fig.6: Autophagy regulates AKAP11-PKA degradation and signaling

27
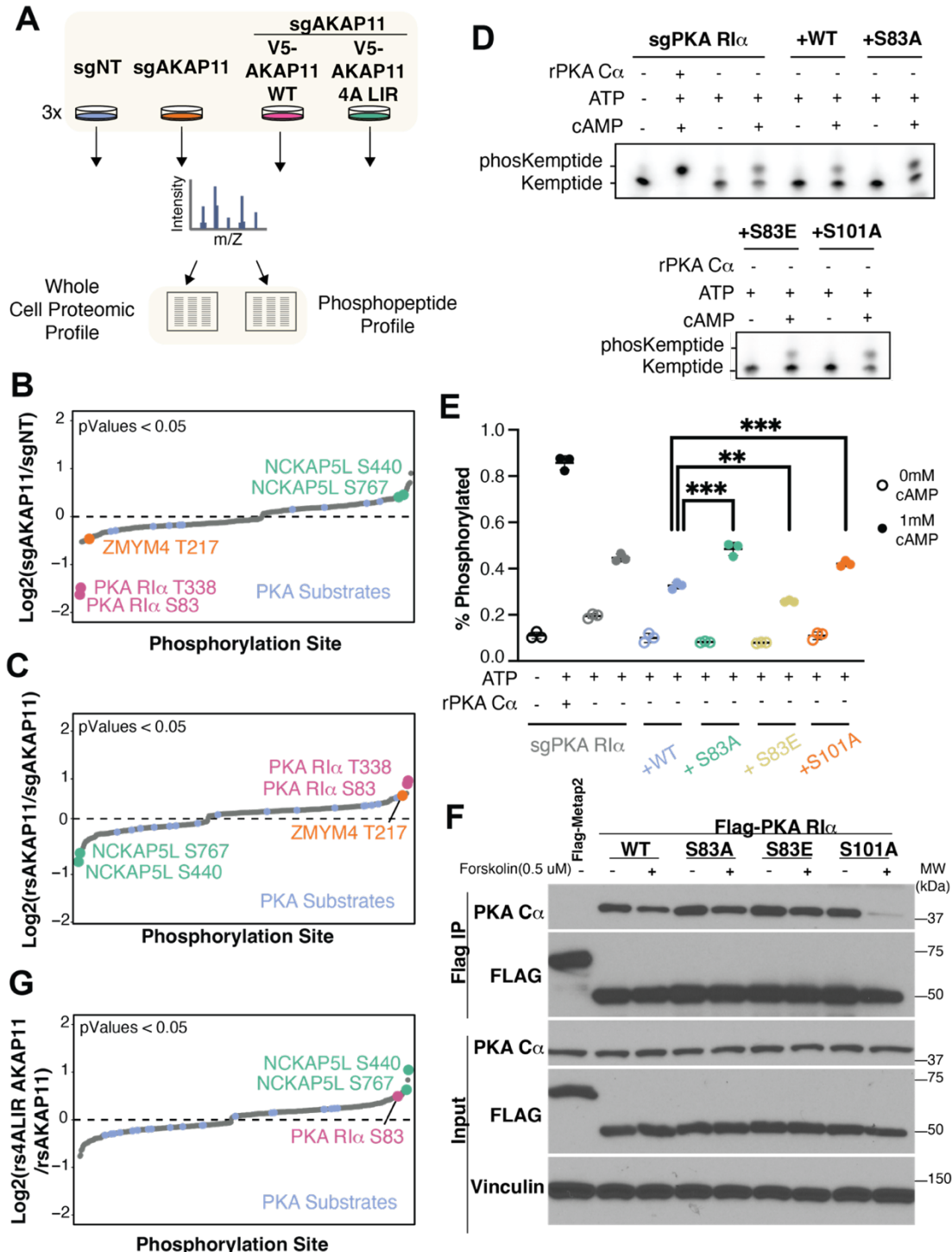
2018; Novero et al., 2024). A fluorescent synthetic peptide encoding for a PKA consensus phosphorylation sequence (LRRASLG) was incubated with cell lysates from RIa-deleted HEK-293T cells that were reconstituted with wild-type, phosphomimetic (S83E) or phospho-null (S83A) RIa constructs. Adding the synthetic PKA substrate peptide to the RIa-deleted lysates resulted in partial, cAMP-stimulated peptide phosphorylation by endogenous Ca present in the lysate (Fig. 6D-6E).

In lysates from cells reconstituted with wild-type RIa, reformation of the PKA holoenzyme partially inhibited Ca activity, leading to significant reduction of the phosphorylated peptide upon cAMP addition (Fig. 6D-6E). The phospho-null S83A mutant was less capable of inhibiting cAMP-induced Ca kinase activity, resulting in more phosphorylated peptide. Conversely, the phospho-mimetic S83E mutant inhibited substrate peptide phosphorylation more potently than wild-type RIa (Fig. 6D-6E). Consistent with a previous report (Haushalter et al., 2018) mutating Ser 101, the target of PKG, to Ala also impaired inhibition of Ca kinase activity by RIa (Fig. 6D-6E).

To determine whether the different peptide phosphorylation efficiencies reflect different strength of association between RIa and Ca, we carried out co-immunoprecipitation experiments between FLAG-tagged, wild-type and mutant RIa, and endogenous Ca (Fig. 6F). These experiments showed that, relative to wild-type RIa, the phosphomimetic S83E RIa mutant had increased binding to Ca in cAMP-stimulated conditions, providing a rationale for the increased potency of this mutant at inhibiting Ca (Fig. 6F). In contrast, we did not detect destabilization of the RIa-Ca interaction by the S83A mutation, likely reflecting a more subtle effect of this mutation.

Because RIa phosphorylation at Ser83 was strongly decreased in AKAP11-depleted cells, AKAP11 may favor interaction of the bound PKA holoenzyme with an S83-phosphorylating upstream kinase (see Discussion). The phosphoproteomic analysis also provided hints to the role of the LIR motif of AKAP11 in regulating the activity of the PKA holoenzyme bound to it. Ser83 phosphorylation was significantly increased in AKAP11-deleted cells reconstituted with AKAP11[4ALIR] mutant compared to AKAP11[WT]-reconstituted cells, even after normalizing for the total levels of RIa protein (Fig. 6G). Given that S83 phosphorylation was inhibitory toward PKA kinase activity (Fig. 6D-6E) these data suggest that binding of PKA to ATG8 family proteins may antagonize access to RIa by the Ser83-phosphorylating kinase(s), thereby promoting PKA activation.

The phosphoproteomic analysis in this reconstituted system identified additional AKAP11-dependent signaling events that were regulated by AKAP11 interaction with the autophagic machinery. AKAP11 deletion caused increased phosphorylation of NCK associated protein 5 like (NCKAP5L), a microtubule plus ends-binding protein that regulates microtubule bundling and acetylation (Mori et al., 2015) at two non-PKA sites: Ser440 and Ser767. Both phosphorylation events were suppressed back to control

levels by re-expressing wild-type AKAP11, but not by AKAP11[4ALIR] (Fig. 6B, 6C and 6G). Thus, AKAP11 binding to ATG8 proteins may be required for its ability to promote NCKAP5L dephosphorylation.

Collectively, these data point to a model where binding of AKAP11 to ATG8 proteins regulates its bound PKA holoenzyme in two ways: 1- by regulating 'gating' of bound PKA by an upstream kinase, possibly amplifying the effect of local cAMP 2- by promoting autophagic degradation of the entire complex. Both processes are required for the correct phosphorylation of both PKA-dependent and independent sites, resulting in the fine-tuning of a vast signaling program that may play important roles in neuronal cell homeostasis (Fig. 7).
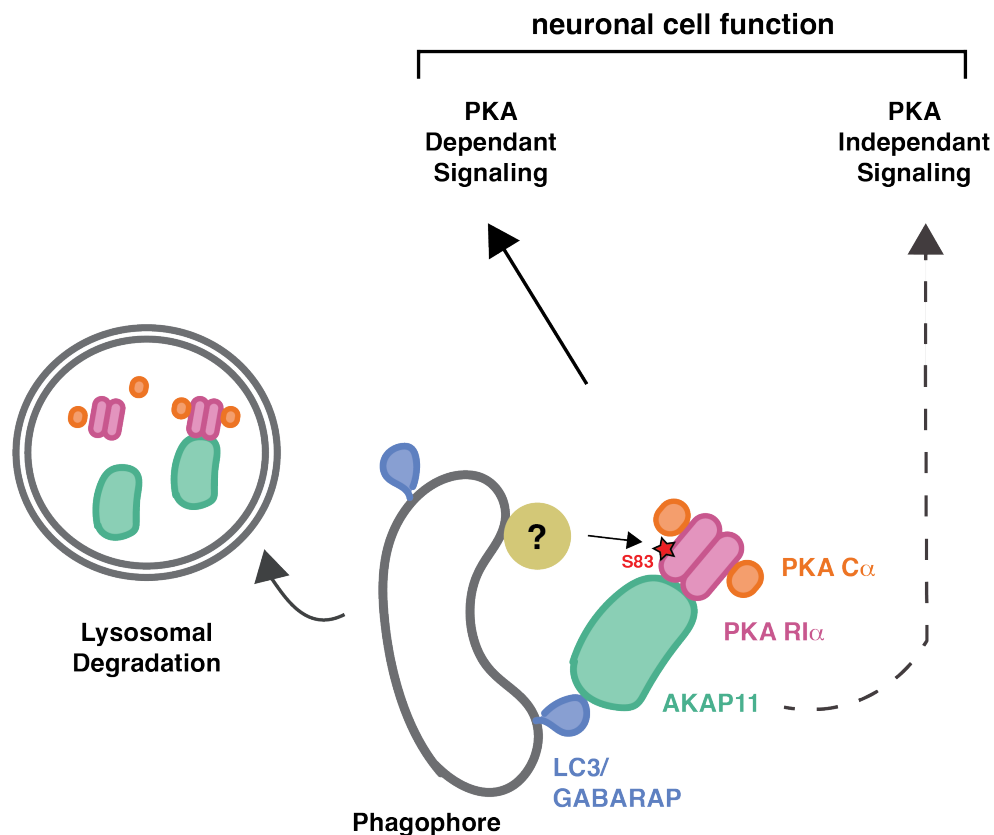
Discussion

We undertook this study with the initial goal of identifying multiprotein signaling complexes targeted by autophagy for degradation. Our lysosomal immunoisolation and proteomics identified the AKAP11-bound PKA holoenzyme as the prominent kinase complex targeted for autophagic degradation. Through follow-up functional experiments and phosphoproteomics, we uncover new molecular functions of AKAP11, provide insights into how its autophagic capture modulates PKA signaling, and begin to shed

29

light on how loss of AKAP11, an event strongly linked to the pathogenesis of SCZ/BP, impacts phosphorylation events inside neuronal cells.

Our combined lysosomal proteomics, co-IP and imaging experiments establish with high confidence that AKAP11 mediates the autophagic degradation of a PKA holoenzyme that includes both RIa and Ca, as opposed to RIa only as previously suggested (Deng et al., 2021; Overhoff et al., 2022; X. Zhou et al., 2024). This is to be
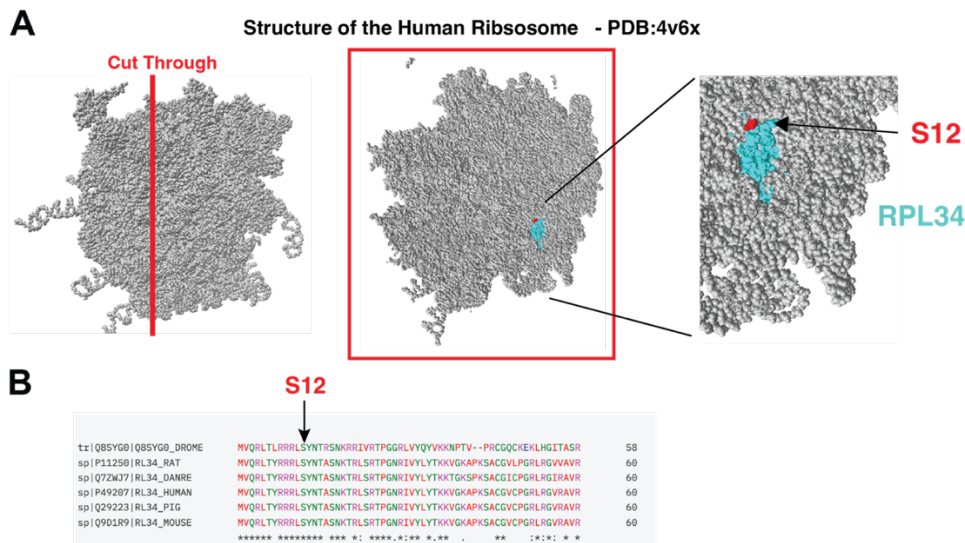
expected in light of evidence that, even under cAMP concentrations leading to full PKA activation, a significant fraction of Ca remains associated with RIa (Smith et al., 2013, 2017). Whereas AKAP11 and RIa directly bind to each other, Ca associates with AKAP11 via its cAMP-regulated interaction with RIa, explaining why AKAP11 depletion led to higher stabilization of RIa protein levels relative to Ca.

As a physical scaffold for PKA, one expected function of AKAP11 is to bring the PKA holoenzyme in proximity to specific substrate proteins, facilitating their phosphorylation upon local elevation of cAMP levels and de-inhibition of bound Ca. Previous reports indeed support this role for AKAP11 (Logue, Whiting, Tunquist, Langeberg, et al., 2011; Whiting et al., 2015). However, our results identify two additional functions of AKAP11. One is its ability to cause degradation of its bound RIa and Ca in autophagosomes; the second is to enable regulatory phosphorylation of its bound RIa by one or more upstream kinases, leading to stronger inhibition of Ca. The scaffolding function predicts that ablation of AKAP11 should lead to decreased phosphorylation of a subset of PKA substrates, whereas the pro-autophagic and RIa-regulating functions predict increased phosphorylation of certain PKA substrates upon AKAP11 loss (Fig. 7).

Indeed, our phosphoproteomic experiments in i3 neurons show that AKAP11 loss increased phosphorylation of some canonical PKA substrates, while decreasing

phosphorylation of others (Fig. 5D and supplementary data 2). Among the most hypophosphorylated PKA substrates upon AKAP11 depletion was Ser12 of RPL34; we speculate that AKAP11 may bring the RIa- Ca in proximity to RPL34 at some point during the life cycle of the ribosomal large subunit, thus favoring Ser12 phosphorylation.

Conversely, in AKAP11-defective cells the total levels of RIa and, to a lesser degree, Ca were increased, whereas the inhibitory phosphorylation of Ser83 on RIa was decreased. Combined, these effects may result in association of more numerous, overactive holoenzyme molecules with other AKAP proteins, leading to hyperphosphorylation of other PKA substrates. Indeed, depleting AKAP11 from i3 neurons led to increased phosphorylation of canonical PKA sites on multiple proteins. Thus, AKAP11 emerges as a modulator that, via its scaffolding and autophagic adaptor functions, shapes both the strength and specificity of PKA signaling toward distinct classes of substrates.

Ser83 on RIa scored as the top AKAP11-dependent phosphorylated site. Although Ser83 is not in the IS segment, it lies nearby in a flexible loop that is not resolved in the numerous published structures of RIA but can be visualized in Alphafold predictions (Fig. S3C). Though the exact molecular details of how Ser83 phosphorylation alters PKA activity is difficult to determine without structural information, the Alphafold model suggests that a phospho-group on Ser83 side chain may alter the packing of this flexible loop against PKA Ca, possibly forming a salt bridge with nearby Arg257 and thus stabilizing the interaction with the catalytic subunit.

C AlphaFold PKA RIα - PKA Cα Complex Prediction

WT PKA RIα — S83, R257

S83E PKA RIα — S83E, R257

PKA RIα
PKA Cα
Inhibitory Site

D

S83

```
sp|Q5I0F6|KAP0_DANRE    EAKQMVSQQKSSSRSDSREDEVS--PPMNPVVKGRRRRGAISAEVYTEEDATSYVRKVIP  117
sp|Q5ZM91|KAP0_CHICK    ETKQLLNQQKSGSRSDSREDEISPPPPMNPVVKGRRRRGAISAEVYTEEDAASYVRKVIP  120
sp|P00514|KAP0_BOVIN    EAKQIQNLQKAGSRADSREDEISPPPP-NPVVKGRRRRGAISAEVYTEEDAASYVRKVIP  118
sp|P10644|KAP0_HUMAN    EAKQIQNLQKAGTRTDSREDEISPPPP-NPVVKGRRRRGAISAEVYTEEDAASYVRKVIP  119
sp|P09456|KAP0_RAT      EARQIQSLQKSGIRTDSREDEISPPPP-NPVVKGRRRRGAISAEVYTEEDAASYVRKVIP  119
sp|Q9DBC7|KAP0_MOUSE    EARQIQCLQKTGIRTDSREDEISPPPP-NPVVKGRRRRGAISAEVYTEEDAASYVRKVIP  119
                        *::*:  **:. *:******:*  ** *********************:********
```

How AKAP11 promotes RIa phosphorylation on Ser83 remains to be determined. Based on high-throughput profiling of human S/T kinase specificity (J. L. Johnson et al., 2023), Ser83 is a target site for Kinase Interacting with Stathmin (KIS), several Tyrosine kinase-like (TKL) including Activin receptor type-1B (ACVR1B) and Bone morphogenetic protein receptor type-2 (BMPR2), as well as the Casein Kinase (CK) group including CKId and CKIg2. Conceivably, AKAP11 may bind to one or more of these kinases, holding them in physical proximity to the RIa linker-hinge region. Our observation that, in cells expressing the AKAP11[4ALIR] mutant, S83 phosphorylation was increased after normalizing for total RIa levels suggests that binding of AKAP11 to ATG8 family proteins may somehow regulate access of S83-phosphorylating kinases to their RIa substrate proteins. Further studies will clarify the relationship between these two binding events.

Our data do not support a previously proposed model where selective autophagic degradation of RIa frees up Ca in order to amplify PKA signaling (Deng et al., 2021; Overhoff et al., 2022). First, under all paradigms tested we found that a pool of cellular Ca was degraded along with R1a in an autophagy- and AKAP11-dependent manner, the only exception being when we induced cAMP levels that are considered supra-physiological (Figs 1-4). This finding is in line with reports that the R- and C-subunits remain associated, at least in part, under conditions where PKA is catalytically active (Smith et al., 2013, 2017). Second, ablation of AKAP11 in i3 neurons and HEK-293T cells did not uniformly lead to suppression of PKA signaling, instead it resulted in some substrates being hyperphosphorylated, while others were hypophosphorylated. (Figs 5-6). These results indicate that AKAP11-dependent autophagic degradation of RIa is not a general 'brake-release' mechanism for PKA signaling.

It should be pointed out that, in previous studies connecting autophagy to PKA regulation, no phosphoproteomic analysis of AKAP11-deficient cells were carried out. Instead, the phosphoproteomes of wild-type versus autophagy-impaired cells were compared (Overhoff et al., 2022; X. Zhou et al., 2024). Given its pleiotropic roles, autophagy may control PKA signaling through both AKAP11-dependent and independent mechanisms, thus providing a rationale for the significant differences between those studies and ours. Moreover, conditions that stimulate autophagy, such as glucose withdrawal (Deng et al., 2021) or amino acid starvation (Overhoff et al., 2022) could bias AKAP11-degradation toward RIa and away from Ca, but whether and how this occurs remains to be determined.

Our phosphoproteomic analysis reveals that the signaling functions of AKAP11 go well beyond direct regulation of PKA. In the i3 neuron model, close to 95% of differentially phosphorylated peptides were non-PKA substrates. Some of these altered phosphorylation events may be indirectly linked to dysregulated PKA. However, given the ability of AKAP11 to scaffold other signaling proteins such as GSK3b and PP1,

AKAP11-dependent but PKA-independent regulatory actions are likely and must be taken into account when considering how AKAP11 gene loss may alter neuronal cell homeostasis and circuitry, leading to SZ/BP. Notably, our proteomic-based lysosome profiling did not detect GSK3β or PP1 as autophagic substrates (Fig.1 and supplementary data 1); thus, a possible function of AKAP11-dependent autophagy may be to eliminate AKAP11-PKA complexes that are unassembled with the other components of this signaling supercomplex, thus helping maintain its correct composition and stoichiometry.

Materials

Antibodies and Chemicals
Reagents were obtained from the following sources: antibodies to AKAP11 (LS-C374339-100) from LSBio. FLAG (#14793), HA (#3724) PKA RI-α (D54D9) (#5675), PKA C-α (D38C6) (#5842), phospho-PKA substrate (#9624), LC3B (D11) (#3868), Vinculin (E1E9V) (#13901), TAX1BP1 (D1D5)(#13901), V5 rabbit (#13202), V5 mouse (#80076), SQSTM1/p62 (#397749), PP2AA (#2041), HOP (#5670), eEF1A (#2551), CACYBP (#3354), HSP90 (#4874), CCT2 (#3561), PSMA2 (#11864), PP2AC (#2259), GPI (#57893), GSK3β (#12456), Synapsin (#4297), Oct4 (#27505) from Cell Signaling Technologies. VAPA (15275-1-AP), SQSTM1/p62 (18420-1-AP), eEF1D (10630-1-AP), CCT5 (67400-1-Ig), MAP2 (17490-1-AP) from Proteintech. GFP (SC-9996), LAMP2 (SC-18822) from Santa Cruz Biotechnology. VAPB(A0302-894A), ORP11 (A304-581A) from Bethyl Laboratories. GFP (A11122) from Invitrogen, PSMD7 (ab11436) from Abcam, PKAR2A (VPA00905) from BioRad, Tuj1 from Biolegend (801202). Bafilomycin A1 (Alfa Aesar, J61835), Torin1 (Tocris, 4247), Forskolin, Lenti-X concentrator (Takara Bio #631232). GFP-trap (gta) and mNeonGreen-trap (nta) from Proteintech/Chromotek. Pierce Anti-HA magnetic beads (88837) from Thermo Scientific. Anti-Flag beads

Methods

Mammalian Cell Culture
HEK293T cells and their derivatives were cultured in DMEM base media with 10% fetal bovine serum (FBS) and supplemented with 2mM Glutamine, and 1% penicillin and streptomycin. All cell lines were cultured at 37°C and 5% CO_2. All cell lines were free of

mycoplasma contamination, routinely checked by mycoplasma PCR Detection Kit (abm, #G238) and/or DAPI staining.

Lentivirus production and infection

Lentiviruses were made by co-transfecting pLJM1 constructs with psPAX2 and pMD2G packaging plasmids into HEK293T cells using PEI transfection reagent. Viral supernatant was collected after 48 hours and again after 72 hours post-transfection and filtered using 0.45 μm syringe filter. The collected virus was concentrated using Lenti-X concentrator (Takara Bio #631232) according to manufacturer's protocol and stored at - 80°C. For lentivirus transfection, target cells were seeded along with the virus and 10ug/mL polybrene. After 24 hour incubation, virus containing media was removed and fresh media containing puromycin(1 μg/mL) hygromycin (200 μg/mL), or blasticidin (5 μg/mL) was added for selection.

Drug Treatments

All drug treatments were performed as follows unless otherwise
specified. Bafilomycin A1 (Alfa Aesar, J61835) was used at 500 nM for 5 hours. Torin1 (Tocris, 4247) was used at 250 nM for 1 hour. Forskolin was used at 1 μM for 25 minutes.

Generation of CRISPR Knockout cell lines

HEK293T sgATG7 were generated as described previously (Abu-Remaileh M et al. 2017), sgFIP200 were generated as described previously (An, H. et al. 2020).
To generate HEK293T sgAKAP11, sgPRKAR1A, the following targeting sequences were cloned into pLentiCRISPRv2 vector: AKAP11-5'- ATGTCCCAGGACATTCACTG-3', PRKAR1A- 5'-ACCAAAAGATTACAAGACAA-3'. Infected cells were selected for hygromycin resistance. Cells were maintained in selection medium for 3-5 days to ensure knockout. Knockouts were validated by immunoblotting and LysoIP.

Generation of CRISPRi i3 Neurons

To generate sgAKAP11 KD i3 Neurons, the following target sequences were cloned into pLG15 vector plasmid: sgNT 5'-GTCCACCCTTATCTAGGCTA-3',sgAKAP11[#1] 5'-AGCCTCCGCGGCGAGCACGT-3', sgAKAP11[#3] 5'-GGTGACATGTCTGTGAGCTG-3', sgAKAP11[#5] 5'- TCGGCGCCCGGCTCACCTGG-3'

i[3]Neuron differentiation

CRISPRi- i[3]iPSCs containing neurogenin2 (NGN2) inducible cassette and dCas9-BFP-KRAB were a generous gift from Dr. Michael Ward (Tian et.al, 2019). CRISPRi- i[3]iPSCs

were differentiated as previously described (Fernandopulle, 2018). Briefly, iPSCs were dissociated with Accustase (Gibco) and seeded onto matrigel (Corning) coated six-well plates. iPSCs were infected with lentiviruses concentrated in essential-8 medium (Gibco) expressing sgNT or sgAKAP11. After 24 hours, media was replaced with fresh media containing puromycin (1 ug/mL, SUPPLIER). Media was replaced daily with fresh media containing puromycin for 72 hrs. After selection, cells were expanded for one passage before dissociating and seeding cells into induction medium containing N2-supplement (N2,Gibco) in Knockout DMEM/F:12 with non-essential amino acids, GlutaMax and doxycycline (NEAA, Gibco; GlutaMax,Gibco; Doxycycline 2µg/mL,). Media was replaced with fresh induction media for 72 hrs, before dissociating cells and seeding onto PLO/Laminin coated plates (prepared as described in Fernandopulle, 2018) containing BrainPhys neuronal differentiation media supplemented with B27+ containing BDNF, NT-3, and GDNF. i³Neurons were given 60% media changes (remove 50%, add back 60%) every 3 days until harvested for experiments.

Lysosome immunoprecipitation (LysoIP)

Lysosomes from stable cells lines stably expressing TMEM192-RFP-3xHA were purified as previously described (Lim et al. 2019). In brief, cells were 18million cells were seeded in a 15cm dish, the following day cells were treated either with DMSO, 500nM BAFA1 for 5 hours or $20\mu M$ Leupeptin + $20\mu M$ Pepstatin for 24 hours. All following steps were done with cold buffers or on ice to maintain samples at 4C. Cells were washed and then resuspended in 5ml of PBS. Samples were spun at 320xg and pelleted cells were resuspended in 750uL K-PBS (136mM KCl, 10mM KH2PO4, pH7.25, with addition of fresh 0.5mM TCEP and Pierce Protease inhibitor tablet (Thermo A32965) with 3.6% Opti-prep (Sigma D1556). Cells were mechanically lysed by five passages through a 23-gauge needle and post-nuclear fractions were collected after a 1370xg 10min spin and incubated with magnetic anti-HA beads for 20min. Samples were washed 3 times with 1mL of K-PBS using a magnetic stand. For western blot analysis, samples were eluted directly into 2xUrea sample loading buffer (150 mM Tris, pH 6.5, 6 M urea, 6% SDS, 25% glycerol, 5% β-mercaptoethanol, 0.02% bromophenol blue) at room temperature overnight. For proteomics experiments, lysosomal immunoprecipitates were eluted from beads using 0.1% NP-40 in PBS for 30 min at 37°C, beads were removed, and the resulting eluate was snap-frozen with LN2.

LysoIP mass spectrometry and proteomic analysis

Samples were prepared in biological triplicates and analyzed by tandem mass spectrometry with an Orbitrap analyzer by the Proteomics Core Facility at the

Whitehead Institute. The samples were TCA-precipitated, resuspended in TEAB, reduced and alkylated, digested, isotope-labelled, combined, cleaned up (SPE) and fractionated.

The resulting data was filtered to exclude contaminants listed in the cRAP database (common Repository of Adventitious Proteins, GPM) or in MaxQuant, and to include only proteins with peptides occurring in at least two replicates.Consequently, the dataset was normalized in Python: First, based on the mean total intensity per MS run, all MS channels were corrected for sample loading. Second, Internal Reference Scaling (IRS) was the last normalization step. Batchcorrection with Combat's PyCombat served as benchmark. For Principal Component Analysis, the data was standard-scaled. Following normalization, the foldchange between samples was calculated as the log base 2 of the ratio of the averages. Significance for each foldchange was determined by taking the -log base ten of a welch two-tailed t-test.

Bioinformatic analysis

List of lysosomal proteins was obtained experimentally (954 human proteins). Protein interactions between the initial list of lysosomal proteins and other interactors were determined based on BioGRID (https://thebiogrid.org/), a data base of protein-protein interactions from both high-throughput datasets and individual focused studies. The resulting list included the protein-protein interactome of the initial lysosomal protein list. The connectogram was constructed using Cytoscape (https://cytoscape.org/).

Gene ontology analysis was performed using Panther with default settings. The plot was generated in GraphPad Prism. Pathway enrichment analysis in i3 Neurons was performed using Metascape(Y. Zhou et al., 2019). The plots were generated in GraphPad Prism.

Immunofluorescence

Cells were seeded on fibronectin-coated glass coverslips in 6-well or 12-well plates the day before the experiment was to be performed. Cells were Bafilomycin or Torin treated where indicated and fixed using 4% paraformaldehyde (PFA) for 15 minutes at RT. Cells were rinsed 3 times with PBS, permeabilized with 0.1% (w/v) saponin in PBS for 10 minutes at RT. Cells were rinsed in PBS 3 times. Primary antibodies were diluted in 5% normal donkey serum (NDS) (Jackson ImmunoResearch) and incubated at RT for 1 hour. The coverslips were rinsed with PBS 3 times. Coverslips were then incubated in fluorescently-conjugated secondary antibodies diluted to 1:4000 diluted in 5% NDS for 45 minutes at RT while being protected from light. Coverslips were then rinsed with PBS 3 times and mounted on glass slides using VECTASHIELD Antifade Mounting Medium with or without DAPI (Vector labs)

Microscopy

All confocal microscopy was using a spinning-disk confocal system built on a Nikon Eclipse Ti microscope (Nikon Instruments) with Andor Zyla-4.5 sCMOS camera system(Andor Technology) using a Plan Apo 60× oil objective. Images of fine cellular detail were acquired with an additional 1.5× magnifier.

Image Analysis

For quantification of co-localization, 5–10 non-overlapping images were acquired from each coverslip. Raw, unprocessed images were imported into ImageJ v1.53 and converted to 8-bit images, and images of individual channels were thresholded independently to exclude background and non-specific staining noise and converted to binary masks. Co-localization analysis was assessed using the threshold 'AND' function. Percent co-localization was calculated by dividing co-localized value by lysosomal marker threshold.

Cell lysis and Co-Immunoprecipitation

Cell lysates were prepared by removing media and rinsing cell monolayer once with DPBS and lysed in either of the following lysis buffers: Triton-based (1% Triton X-100, 10 mM sodium β-glycerol phosphate, 10mM sodium pyrophosphate, 4 mM EDTA, 40 mM HEPES, pH 7.4, and one EDTA-free protease inhibitor tablet per 50 ml) or CHAPS-based (0.3% CHAPS, 10 mM sodium β-glycerol phosphate, 10mM sodium pyrophosphate, 2 mM EDTA, 20 mM HEPES, 150 mM NaCl, pH 7.6, one EDTA-free protease inhibitor tablet per 50 ml). Cells lysed on nutator for 10 minutes. Lysates were cleared via centrifugation using a microcentrifuge at 17,000xg for 10 minutes at 4°C. Protein content in lysate samples were measured by Bradford assay or BCA. Samples of equal protein concentration and addition of 5X SDS sample buffer (235mM Tris, pH 6.8, 10% SDS, 25% Glycerol 25% β-mercaptoethanol, 0.1%bromophenol blue) were prepared for SDS-PAGE.

For Flag or HA immunoprecipitations, cells were seeded in a 10cm at a density appropriate for them to reach confluency after 24h. Cells were lysed as described above. 25 μl of a well-mixed 50% slurry of anti-Flag M2 affinity gel or HA magnetic beads were added to each lysate sample and incubated at 4°C while on the rotator for 1 hour. For GFP or mNeonGreen IP, 15 μl of well-mixed 50% slurry of GFP-Trap agarose or mNeonGreen-Trap agarose were added to each lysate sample and incubated at 4°C while on the rotator for 1 hour. Immunoprecipitant beads were washed three times with

lysis buffer. Immunoprecipitated proteins were denatured by adding 100μl of sample buffer, left overnight at RT or heating to 95°C for 5 minutes.

For GFP-LC3 and GFP-GABARAP competition assay in cells, immunoprecipitation was carried out as described above except cells were lysed in 0.3% CHAPS buffer, containing the LIR peptides (500 μM). Lysates were incubated at 4°C for 1.5 hours before incubating with GFP-trap agarose (10 μl) for 30 minutes.

Immunoblotting
For immunoprecipitation, 10% of the total immunoprecipitated material was loaded per lane, and 0.5% of total input was loaded per lane. Proteins were transferred to a PVDF membrane (Millipore IPVH00010), blocked with 5% non-fat milk in TBS-T, and incubated in primary antibodies (diluted in 5% milk in TBS-T) for 3 hours at RT or overnight at 4°C. Membranes were rinsed with TBS-T and incubated with horseradish peroxidase conjugated anti-rabbit or anti-mouse secondary antibodies (diluted in 5% milk in TBS-T) for 1 h at room temperature. Membranes were washed again with TBS-T and incubated with Pierce ECL Western Blotting Substrate (Thermo Scientific, 32109) before being exposed to Prometheus ProSignal Blotting Film (Genesee Scientific, 30-507L).

Phosphoproteomic sample preparation
HEK293T sgNT or sgAKAP11 and sgAKAP11 stably expressing V5-AKAP11 WT or V5-AKAP11 dLIR were seeded (5.0 x10^6 cells) in 10cm dish in DMEM complete medium (DMEM, 10% FBS, 2mM Glutamine, 1% penicillin/streptomycin). After overnight adherence cells were switched to DMEM + 10% dFBS medium. Cells were harvested 24 hours later and lysed as previously described. Protein content in lysate samples were measured by BCA. Lysis was flash frozen in liquid nitrogen until mass spectrometry analysis.

Phosophoproteomic Mass spectrometry
All samples were labeled with iodoacetamide, and resuspended in 100mM of 4-(2-Hydroxyethyl)-1-piperazinepropanesulfonic acid (EPPS) buffer, pH 8.5 and digested at 37C with trypsin overnight. The samples were labeled with TMT Pro and, quenched with hydroxylamine. All the samples were combined and desalted using a 100mg Sep-Pak cartridge, followed by drying in a rotary evaporator. Phosphopeptides were enriched using a Fe-NTA spin column (Thermo Fisher). Flow through samples were dried, and fractionated with basic pH reversed phase (BPRP) high-performance liquid

chromatography (HPLC) as described previously. Samples were desalted via StageTip and dried with speedvac. Samples were resuspended in 5% formic acid, and 5% acetonitrile for LC-MS/MS analysis. Mass spectrometry data were collected using Exploris 480 or Orbitrap Eclipse mass spectrometers (Thermo Fisher Scientific) coupled with a nLC-1200 or Vanquish Neo liquid chromatograph (Thermo Fisher Scientific), respectively, with a 90 or 150 min gradient across a Nano capillary column (100μm D) packed with ~35cm of Accucore C18 resin (Thermo Fisher Scientific). A FAIMSPro (Thermo Fisher Scientific) was utilized for field asymmetric waveform ion mobility spectrometry (FAIMS) ion separations. The instrument methods, which are embedded in the RAW files, included Orbitrap MS1 scans (resolution of 120000; mass range 400-1600 m/z; automatic gain control (AGC) target $4\text{x}10^5$, max injection time of 50 ms. MS2 scan parameters were set as described previously (CID collision energy 35%; AGC target 7.5×10^3; rapid scan mode; max injection time (50mM)).

All samples were labeled with iodoacetamide, and resuspended in 100mM of 4-(2-Hydroxyethyl)-1-piperazinepropanesulfonic acid (EPPS) buffer, pH 8.5 and digested at 37C with trypsin overnight. The samples were labeled with TMT Pro and, quenched with hydroxylamine. All the samples were combined and desalted using a 100mg Sep-Pak cartridge, followed by drying in a rotary evaporator. Phosphopeptides were enriched using a Fe-NTA spin column (Thermo Fisher). Flow through samples were dried, and fractionated with basic pH reversed phase (BPRP) high-performance liquid chromatography (HPLC) as described previously. Samples were desalted via StageTip and dried with speedvac. Samples were resuspended in 5% formic acid, and 5% acetonitrile for LC-MS/MS analysis. Mass spectrometry data were collected using Exploris 480 or Orbitrap Eclipse mass spectrometers (Thermo Fisher Scientific) coupled with a nLC-1200 or Vanquish Neo liquid chromatograph (Thermo Fisher Scientific), respectively, with a 90 or 150 min gradient across a Nano capillary column (100μm D) packed with ~35cm of Accucore C18 resin (Thermo Fisher Scientific). A FAIMSPro (Thermo Fisher Scientific) was utilized for field asymmetric waveform ion mobility spectrometry (FAIMS) ion separations. The instrument methods, which are embedded in the RAW files, included Orbitrap MS1 scans (resolution of 120000; mass range 400-1600 m/z; automatic gain control (AGC) target $4\text{x}10^5$, max injection time of 50 ms. MS2 scan parameters were set as described previously (CID collision energy 35%; AGC target 7.5×10^3; rapid scan mode; max injection time (50mM)).

Phosphoproteomics Analysis
Comparative phospho-peptide analysis between genotypes was conducted by first normalizing each phospho-peptide to account for differences in total protein abundance

in each genotype. As such, the relative abundance of each protein at the whole cell level in each genotype was compared to the levels in sgNT control samples then this normalized abundance was used to normalize the corresponding phosphopeptide for each replicate. Following normalization, the foldchange between samples was calculated as the log base 2 of the ratio of the averages. Significance for each foldchange was determined by performing a welch two-tailed t-test. Phosphopeptides foldchanges with pvalues < 0.05 were then plotted on a waterfall plot. All analysis was done using custom R scripts.

Statistical analysis

All graphs were assembled, and statistics were performed using Prism 10 (GraphPad). Error bars on all graphs are shown as the mean ± SEM. The details of each statistical test performed are given in the legend accompanying each figure. Unless otherwise indicated, all co-localization analysis was performed on 10 non-overlapping fields that contain a minimum of 3 cells per field. Unless otherwise indicated, all proteomic measurements were performed on three independent biological replicates for each sample.

Kinase Activity Assay

HEK293T-sgPKA RIa cells were seeded in 6cm tissue culture-treated plates. After overnight incubation, cells were transiently transfected with 5μg Flag-RIa WT type and mutant DNA using PEI, as described previously. 24 hours post transfection, cells were lysed in the plate using 120ul of cold NDP-40 Lysis buffer (1X PBS, 1% NDP-40, 1X PhosStop, 1X EDTA-free protease inhibitor). Lysates were cleared via centrifugation using a microcentrifuge at 17,000xg for 10 minutes at 4°C and then normalized to 2μg/μL. Each kinase reaction was made by using a previously described protocol with final concentrations of 200mM Tris-HCl pH 7.4, 10mM $MgCl_2$, 0.2mM ATP, 0.5mM TCEP, 1X EDTA-Free protease inhibitor, 1X PhosStop, 21uM 5'FAM-Kemptide (Anaspec) and 0.4 μg/μL cell lysate. 1mM cAMP was added where noted. Kinase reactions were incubated at RT for 20 minutes, followed by the addition of 5X SDS sample buffer (235mM Tris, pH 6.8, 10% SDS, 25% Glycerol 25% β-mercaptoethanol, 0.1% bromophenol blue). 2.5uL of each sample were run on 12% NuPAGE Bis-Tris protein gels with MES running buffer. Blank lanes were left in between each sample lane and no protein ladder standard was used.

In-gel fluorescence was imaged using ChemiDoc. Fiji was used for quantification of fluorescence. Background subtraction was performed using a 50-pixel rolling ball

subtraction followed by intensity measurements for each individual band. Percentage of substrate phosphorylated was calculated as phosphorylated intensity/(phosphorylated intensity + unphosphorylated intensity).

References

Abu-Remaileh, M., Wyant, G. A., Kim, C., Laqtom, N. N., Abbasi, M., Chan, S. H., Freinkman, E., & Sabatini, D. M. (2017). Lysosomal metabolomics reveals V-ATPase- and mTOR-dependent regulation of amino acid efflux from lysosomes. *Science (New York, N.Y.)*, *358*(6364), 807–813. https://doi.org/10.1126/science.aan6298

Adriaenssens, E., Ferrari, L., & Martens, S. (2022). Orchestration of selective autophagy by cargo receptors. *Current Biology: CB*, *32*(24), R1357–R1371. https://doi.org/10.1016/j.cub.2022.11.002

Anger, A. M., Armache, J.-P., Berninghausen, O., Habeck, M., Subklewe, M., Wilson, D. N., & Beckmann, R. (2013). Structures of the human and Drosophila 80S ribosome. *Nature*, *497*(7447), 80–85. https://doi.org/10.1038/nature12104

Aryal, S., Bonanno, K., Song, B., Mani, D. R., Keshishian, H., Carr, S. A., Sheng, M., & Dejanovic, B. (2023). Deep proteomics identifies shared molecular pathway alterations in synapses of patients with schizophrenia and bipolar disorder and mouse model. *Cell Reports*, *42*(5), 112497. https://doi.org/10.1016/j.celrep.2023.112497

Ben-Sahra, I., Howell, J. J., Asara, J. M., & Manning, B. D. (2013). Stimulation of de novo pyrimidine synthesis by growth signaling through mTOR and S6K1. *Science (New York, N.Y.)*, *339*(6125), 1323–1328. https://doi.org/10.1126/science.1228792

Ben-Sahra, I., Hoxhaj, G., Ricoult, S. J. H., Asara, J. M., & Manning, B. D. (2016). mTORC1 induces purine synthesis through control of the mitochondrial tetrahydrofolate cycle. *Science (New York, N.Y.)*, *351*(6274), 728–733. https://doi.org/10.1126/science.aad0489

Bock, A., Irannejad, R., & Scott, J. D. (2024). cAMP signaling: A remarkably regional affair. *Trends in Biochemical Sciences*, *49*(4), 305–317. https://doi.org/10.1016/j.tibs.2024.01.004

Boeshans, K. M., Resing, K. A., Hunt, J. B., Ahn, N. G., & Shabb, J. B. (1999). Structural characterization of the membrane-associated regulatory subunit of type I cAMP-dependent protein kinase by mass spectrometry: Identification of Ser81 as the in vivo phosphorylation site of RIalpha. *Protein Science: A Publication of the Protein Society*, *8*(7), 1515–1522. https://doi.org/10.1110/ps.8.7.1515

Boya, P., Reggiori, F., & Codogno, P. (2013). Emerging regulation and functions of autophagy. *Nature Cell Biology*, *15*(7), 713–720. https://doi.org/10.1038/ncb2788

Brunn, G. J., Hudson, C. C., Sekulić, A., Williams, J. M., Hosoi, H., Houghton, P. J., Lawrence, J. C., & Abraham, R. T. (1997). Phosphorylation of the translational repressor PHAS-I by the mammalian target of rapamycin. *Science (New York, N.Y.)*, *277*(5322), 99–101. https://doi.org/10.1126/science.277.5322.99

Bruystens, J. G., Wu, J., Fortezzo, A., Del Rio, J., Nielsen, C., Blumenthal, D. K., Rock, R., Stefan, E., & Taylor, S. S. (2016). Structure of a PKA RIα Recurrent Acrodysostosis Mutant Explains Defective cAMP-Dependent Activation. *Journal of Molecular Biology*, *428*(24 Pt B), 4890–4904. https://doi.org/10.1016/j.jmb.2016.10.033

Budovskaya, Y. V., Stephan, J. S., Deminoff, S. J., & Herman, P. K. (2005). An evolutionary proteomics approach identifies substrates of the cAMP-dependent protein kinase. *Proceedings of the National Academy of Sciences, 102*(39), 13933–13938. https://doi.org/10.1073/pnas.0501046102

Cherra, S. J., Kulich, S. M., Uechi, G., Balasubramani, M., Mountzouris, J., Day, B. W., & Chu, C. T. (2010). Regulation of the autophagy protein LC3 by phosphorylation. *The Journal of Cell Biology*, *190*(4), 533–539. https://doi.org/10.1083/jcb.201002108

Chino, H., Hatta, T., Natsume, T., & Mizushima, N. (2019). Intrinsically Disordered Protein TEX264 Mediates ER-phagy. *Molecular Cell*, *74*(5), 909-921.e6. https://doi.org/10.1016/j.molcel.2019.03.033

Cho, N. H., Cheveralls, K. C., Brunner, A.-D., Kim, K., Michaelis, A. C., Raghavan, P., Kobayashi, H., Savy, L., Li, J. Y., Canaj, H., Kim, J. Y. S., Stewart, E. M., Gnann, C., McCarthy, F., Cabrera, J. P., Brunetti, R. M., Chhun, B. B., Dingle, G., Hein, M. Y., … Leonetti, M. D. (2022). OpenCell: Endogenous tagging for the cartography of human cellular organization. *Science (New York, N.Y.)*, *375*(6585), eabi6983. https://doi.org/10.1126/science.abi6983

Ciuffa, R., Lamark, T., Tarafder, A. K., Guesdon, A., Rybina, S., Hagen, W. J. H., Johansen, T., & Sachse, C. (2015). The selective autophagy receptor p62 forms a flexible filamentous helical scaffold. *Cell Reports*, *11*(5), 748–758. https://doi.org/10.1016/j.celrep.2015.03.062

Davis, O. B., Shin, H. R., Lim, C.-Y., Wu, E. Y., Kukurugya, M., Maher, C. F., Perera, R. M., Ordonez, M. P., & Zoncu, R. (2021). NPC1-mTORC1 Signaling Couples Cholesterol Sensing to Organelle Homeostasis and Is a Targetable Pathway in Niemann-Pick Type C. *Developmental Cell*, *56*(3), 260-276.e7. https://doi.org/10.1016/j.devcel.2020.11.016

Day, M. E., Gaietta, G. M., Sastri, M., Koller, A., Mackey, M. R., Scott, J. D., Perkins, G. A., Ellisman, M. H., & Taylor, S. S. (2011). Isoform-specific targeting of PKA to multivesicular bodies. *The Journal of Cell Biology*, *193*(2), 347–363. https://doi.org/10.1083/jcb.201010034

Deng, Z., Li, X., Blanca Ramirez, M., Purtell, K., Choi, I., Lu, J.-H., Yu, Q., & Yue, Z. (2021). Selective autophagy of AKAP11 activates cAMP/PKA to fuel mitochondrial metabolism and tumor cell growth. *Proceedings of the National Academy of Sciences*, *118*(14), e2020215118. https://doi.org/10.1073/pnas.2020215118

Düvel, K., Yecies, J. L., Menon, S., Raman, P., Lipovsky, A. I., Souza, A. L., Triantafellow, E., Ma, Q., Gorski, R., Cleaver, S., Vander Heiden, M. G., MacKeigan, J. P., Finan, P. M., Clish, C. B., Murphy, L. O., & Manning, B. D. (2010). Activation of a metabolic gene regulatory network downstream of mTOR complex 1. *Molecular Cell*, *39*(2), 171–183. https://doi.org/10.1016/j.molcel.2010.06.022

Fernandopulle, M. S., Prestil, R., Grunseich, C., Wang, C., Gan, L., & Ward, M. E. (2018). Transcription Factor-Mediated Differentiation of Human iPSCs into Neurons. *Current Protocols in Cell Biology*, *79*(1), e51. https://doi.org/10.1002/cpcb.51

Filteau, M., Diss, G., Torres-Quiroz, F., Dubé, A. K., Schraffl, A., Bachmann, V. A., Gagnon-Arsenault, I., Chrétien, A.-È., Steunou, A.-L., Dionne, U., Côté, J., Bisson, N., Stefan, E., & Landry, C. R. (2015a). Systematic identification of signal integration by protein kinase A. *Proceedings of the National Academy of Sciences*, *112*(14), 4501–4506. https://doi.org/10.1073/pnas.1409938112

Filteau, M., Diss, G., Torres-Quiroz, F., Dubé, A. K., Schraffl, A., Bachmann, V. A., Gagnon-Arsenault, I., Chrétien, A.-È., Steunou, A.-L., Dionne, U., Côté, J., Bisson, N., Stefan, E., & Landry, C. R. (2015b). Systematic identification of signal integration by protein kinase A. *Proceedings of the National Academy of Sciences*, *112*(14), 4501–4506. https://doi.org/10.1073/pnas.1409938112

Gingras, A.-C., Gygi, S. P., Raught, B., Polakiewicz, R. D., Abraham, R. T., Hoekstra, M. F., Aebersold, R., & Sonenberg, N. (1999). Regulation of 4E-BP1 phosphorylation: A novel two-step mechanism. *Genes & Development*, *13*(11), 1422–1437.

Goodall, E. A., Kraus, F., & Harper, J. W. (2022). Mechanisms Underlying Ubiquitin-driven Selective Mitochondrial and Bacterial Autophagy. *Molecular Cell*, *82*(8), 1501–1513. https://doi.org/10.1016/j.molcel.2022.03.012

Grisan, F., Iannucci, L. F., Surdo, N. C., Gerbino, A., Zanin, S., Di Benedetto, G., Pozzan, T., & Lefkimmiatis, K. (2021). PKA compartmentalization links cAMP signaling and autophagy. *Cell Death and Differentiation*, *28*(8), 2436–2449. https://doi.org/10.1038/s41418-021-00761-8

Gupte, R. S., Traganos, F., Darzynkiewicz, Z., & Lee, M. Y. W. T. (2006). Phosphorylation of RIalpha by cyclin-dependent kinase CDK 2/cyclin E

modulates the dissociation of the RIalpha-RFC40 complex. *Cell Cycle (Georgetown, Tex.), 5*(6), 653–660.

Han, Y. S., Arroyo, J., & Ogut, O. (2013). Human heart failure is accompanied by altered protein kinase A subunit expression and post-translational state. *Archives of Biochemistry and Biophysics, 538*(1), 25–33. https://doi.org/10.1016/j.abb.2013.08.002

Haushalter, K. J., Casteel, D. E., Raffeiner, A., Stefan, E., Patel, H. H., & Taylor, S. S. (2018). Phosphorylation of protein kinase A (PKA) regulatory subunit RIα by protein kinase G (PKG) primes PKA for catalytic activity in cells. *The Journal of Biological Chemistry, 293*(12), 4411–4421. https://doi.org/10.1074/jbc.M117.809988

Herzog, L. E., Wang, L., Yu, E., Choi, S., Farsi, Z., Song, B. J., Pan, J. Q., & Sheng, M. (2023). Mouse mutants in schizophrenia risk genes GRIN2A and AKAP11 show EEG abnormalities in common with schizophrenia patients. *Translational Psychiatry, 13*, 92. https://doi.org/10.1038/s41398-023-02393-7

Hilger, D., Masureel, M., & Kobilka, B. K. (2018). Structure and dynamics of GPCR signaling complexes. *Nature Structural & Molecular Biology, 25*(1), 4–12. https://doi.org/10.1038/s41594-017-0011-7

Hoyer, M. J., Capitanio, C., Smith, I. R., Paoli, J. C., Bieber, A., Jiang, Y., Paulo, J. A., Gonzalez-Lozano, M. A., Baumeister, W., Wilfling, F., Schulman, B. A., & Harper, J. W. (2024). Combinatorial selective ER-phagy remodels the ER during neurogenesis. *Nature Cell Biology, 26*(3), 378–392. https://doi.org/10.1038/s41556-024-01356-4

Hurley, J. H., & Young, L. N. (2017). Mechanisms of Autophagy Initiation. *Annual Review of Biochemistry, 86*, 225–244. https://doi.org/10.1146/annurev-biochem-061516-044820

Ichimura, Y., Kumanomidou, T., Sou, Y., Mizushima, T., Ezaki, J., Ueno, T., Kominami, E., Yamane, T., Tanaka, K., & Komatsu, M. (2008). Structural basis for sorting mechanism of p62 in selective autophagy. *The Journal of Biological Chemistry, 283*(33), 22847–22857. https://doi.org/10.1074/jbc.M802182200

Isobe, K., Jung, H. J., Yang, C.-R., Claxton, J., Sandoval, P., Burg, M. B., Raghuram, V., & Knepper, M. A. (2017). Systems-level identification of PKA-dependent signaling in epithelial cells. *Proceedings of the National Academy of Sciences, 114*(42), E8875–E8884. https://doi.org/10.1073/pnas.1709123114

Johnson, J. L., Yaron, T. M., Huntsman, E. M., Kerelsky, A., Song, J., Regev, A., Lin, T.-Y., Liberatore, K., Cizin, D. M., Cohen, B. M., Vasan, N., Ma, Y., Krismer, K., Robles, J. T., van de Kooij, B., van Vlimmeren, A. E., Andrée-Busch, N., Käufer, N. F., Dorovkov, M. V., … Cantley, L. C. (2023). An atlas of substrate specificities

for the human serine/threonine kinome. *Nature*, *613*(7945), 759–766. https://doi.org/10.1038/s41586-022-05575-3

Johnson, S. C., Rabinovitch, P. S., & Kaeberlein, M. (2013). mTOR is a key modulator of ageing and age-related disease. *Nature*, *493*(7432), 338–345. https://doi.org/10.1038/nature11861

Kandel, E. R. (2012). The molecular biology of memory: cAMP, PKA, CRE, CREB-1, CREB-2, and CPEB. *Molecular Brain*, *5*, 14. https://doi.org/10.1186/1756-6606-5-14

Kaur, J., & Debnath, J. (2015). Autophagy at the crossroads of catabolism and anabolism. *Nature Reviews. Molecular Cell Biology*, *16*(8), 461–472. https://doi.org/10.1038/nrm4024

Kim, C., Cheng, C. Y., Saldanha, S. A., & Taylor, S. S. (2007). PKA-I Holoenzyme Structure Reveals a Mechanism for cAMP-Dependent Activation. *Cell*, *130*(6), 1032–1043. https://doi.org/10.1016/j.cell.2007.07.018

Kirkin, V., & Rogov, V. V. (2019). A Diversity of Selective Autophagy Receptors Determines the Specificity of the Autophagy Pathway. *Molecular Cell*, *76*(2), 268–285. https://doi.org/10.1016/j.molcel.2019.09.005

Krebs, E. G. (1989). Role of the Cyclic AMP—Dependent Protein Kinase in Signal Transduction. *JAMA*, *262*(13), 1815–1818. https://doi.org/10.1001/jama.1989.03430130091040

Kritzer, M. D., Li, J., Dodge-Kafka, K., & Kapiloff, M. S. (2012). AKAPs: The architectural underpinnings of local cAMP signaling. *Journal of Molecular and Cellular Cardiology*, *52*(2), 351–358. https://doi.org/10.1016/j.yjmcc.2011.05.002

Kuma, A., & Mizushima, N. (2010). Physiological role of autophagy as an intracellular recycling system: With an emphasis on nutrient metabolism. *Seminars in Cell & Developmental Biology*, *21*(7), 683–690. https://doi.org/10.1016/j.semcdb.2010.03.002

Kuo, C. J., Chung, J., Fiorentino, D. F., Flanagan, W. M., Blenis, J., & Crabtree, G. R. (1992). *Rapamycin selectively inhibits interleukin-2 activation of p70 56 kinase*. *358*.

Lamark, T., & Johansen, T. (2021). Mechanisms of Selective Autophagy. *Annual Review of Cell and Developmental Biology*, *37*, 143–169. https://doi.org/10.1146/annurev-cellbio-120219-035530

Lamark, T., Perander, M., Outzen, H., Kristiansen, K., Øvervatn, A., Michaelsen, E., Bjørkøy, G., & Johansen, T. (2003). Interaction codes within the family of mammalian Phox and Bem1p domain-containing proteins. *The Journal of Biological Chemistry*, *278*(36), 34568–34581. https://doi.org/10.1074/jbc.M303221200

Lefkimmiatis, K., & Zaccolo, M. (2014). cAMP signaling in subcellular compartments. *Pharmacology & Therapeutics*, *143*(3), 295–304. https://doi.org/10.1016/j.pharmthera.2014.03.008

Liu, D., Meyer, D., Fennessy, B., Feng, C., Cheng, E., Johnson, J. S., Park, Y. J., Rieder, M.-K., Ascolillo, S., de Pins, A., Dobbyn, A., Lebovitch, D., Moya, E., Nguyen, T.-H., Wilkins, L., Hassan, A., Burdick, K. E., Buxbaum, J. D., Domenici, E., … Charney, A. W. (2023). Schizophrenia risk conferred by rare protein-truncating variants is conserved across diverse human populations. *Nature Genetics*, *55*(3), 369–376. https://doi.org/10.1038/s41588-023-01305-1

Liu, G. Y., & Sabatini, D. M. (2020). mTOR at the nexus of nutrition, growth, ageing and disease. *Nature Reviews. Molecular Cell Biology*, *21*(4), 183–203. https://doi.org/10.1038/s41580-019-0199-y

Logue, J. S., Whiting, J. L., Tunquist, B., Langeberg, L. K., & Scott, J. D. (2011). Anchored Protein Kinase A Recruitment of Active Rac GTPase. *The Journal of Biological Chemistry*, *286*(25), 22113–22121. https://doi.org/10.1074/jbc.M111.232660

Logue, J. S., Whiting, J. L., Tunquist, B., Sacks, D. B., Langeberg, L. K., Wordeman, L., & Scott, J. D. (2011). AKAP220 protein organizes signaling elements that impact cell migration. *The Journal of Biological Chemistry*, *286*(45), 39269–39281. https://doi.org/10.1074/jbc.M111.277756

London, E., Bloyd, M., & Stratakis, C. A. (2020). PKA functions in metabolism and resistance to obesity: Lessons from mouse and human studies. *The Journal of Endocrinology*, *246*(3), R51–R64. https://doi.org/10.1530/JOE-20-0035

Ma, X., Lu, C., Chen, Y., Li, S., Ma, N., Tao, X., Li, Y., Wang, J., Zhou, M., Yan, Y.-B., Li, P., Heydari, K., Deng, H., Zhang, M., Yi, C., & Ge, L. (2022). CCT2 is an aggrephagy receptor for clearance of solid protein aggregates. *Cell*, *185*(8), 1325-1345.e22. https://doi.org/10.1016/j.cell.2022.03.005

Mancias, J. D., & Kimmelman, A. C. (2016). Mechanisms of Selective Autophagy in Normal Physiology and Cancer. *Journal of Molecular Biology*, *428*(9, Part A), 1659–1680. https://doi.org/10.1016/j.jmb.2016.02.027

Mancias, J. D., Wang, X., Gygi, S. P., Harper, J. W., & Kimmelman, A. C. (2014). Quantitative proteomics identifies NCOA4 as the cargo receptor mediating ferritinophagy. *Nature*, *509*(7498), 105–109. https://doi.org/10.1038/nature13148

McConnachie, G., Langeberg, L. K., & Scott, J. D. (2006). AKAP signaling complexes: Getting to the heart of the matter. *Trends in Molecular Medicine*, *12*(7), 317–323. https://doi.org/10.1016/j.molmed.2006.05.008

Means, C. K., Lygren, B., Langeberg, L. K., Jain, A., Dixon, R. E., Vega, A. L., Gold, M. G., Petrosyan, S., Taylor, S. S., Murphy, A. N., Ha, T., Santana, L. F., Tasken, K., & Scott, J. D. (2011). An entirely specific type I A-kinase anchoring protein

that can sequester two molecules of protein kinase A at mitochondria. *Proceedings of the National Academy of Sciences*, *108*(48), E1227–E1235. https://doi.org/10.1073/pnas.1107182108

Moll, A., Ramirez, L. M., Ninov, M., Schwarz, J., Urlaub, H., & Zweckstetter, M. (2022). Hsp multichaperone complex buffers pathologically modified Tau. *Nature Communications*, *13*(1), 3668. https://doi.org/10.1038/s41467-022-31396-z

Monterisi, S., & Zaccolo, M. (2017). Components of the mitochondrial cAMP signalosome. *Biochemical Society Transactions*, *45*(1), 269–274. https://doi.org/10.1042/BST20160394

Mori, Y., Inoue, Y., Tanaka, S., Doda, S., Yamanaka, S., Fukuchi, H., & Terada, Y. (2015). Cep169, a Novel Microtubule Plus-End-Tracking Centrosomal Protein, Binds to CDK5RAP2 and Regulates Microtubule Stability. *PloS One*, *10*(10), e0140968. https://doi.org/10.1371/journal.pone.0140968

Nakatogawa, H. (2020). Mechanisms governing autophagosome biogenesis. *Nature Reviews Molecular Cell Biology*, *21*(8), 439–458. https://doi.org/10.1038/s41580-020-0241-0

Neufeld, T. P. (2010). TOR-dependent control of autophagy: Biting the hand that feeds. *Current Opinion in Cell Biology*, *22*(2), 157–168. https://doi.org/10.1016/j.ceb.2009.11.005

Novero, A. G., Curcio, C., Steeman, T. J., Binolfi, A., Krapf, D., Buffone, M. G., Krapf, D., & Stival, C. (2024). A versatile kinase mobility shift assay (KiMSA) for PKA analysis and cyclic AMP detection in sperm physiology (and beyond). *Frontiers in Cell and Developmental Biology*, *12*, 1356566. https://doi.org/10.3389/fcell.2024.1356566

Ohnstad, A. E., Delgado, J. M., North, B. J., Nasa, I., Kettenbach, A. N., Schultz, S. W., & Shoemaker, C. J. (2020). Receptor-mediated clustering of FIP200 bypasses the role of LC3 lipidation in autophagy. *The EMBO Journal*, *39*(24), e104948. https://doi.org/10.15252/embj.2020104948

Omar, M. H., & Scott, J. D. (2020). AKAP Signaling Islands: Venues for Precision Pharmacology. *Trends in Pharmacological Sciences*, *41*(12), 933–946. https://doi.org/10.1016/j.tips.2020.09.007

Overhoff, M., Tellkamp, F., Hess, S., Tolve, M., Tutas, J., Faerfers, M., Ickert, L., Mohammadi, M., De Bruyckere, E., Kallergi, E., Delle Vedove, A., Nikoletopoulou, V., Wirth, B., Isensee, J., Hucho, T., Puchkov, D., Isbrandt, D., Krueger, M., Kloppenburg, P., & Kononenko, N. L. (2022). Autophagy regulates neuronal excitability by controlling cAMP/protein kinase A signaling at the synapse. *The EMBO Journal*, *41*(22), e110963. https://doi.org/10.15252/embj.2022110963

Palmer, D. S., Howrigan, D. P., Chapman, S. B., Adolfsson, R., Bass, N., Blackwood, D., Boks, M. P., Chen, C.-Y., Churchhouse, C., Corvin, A. P., Craddock, N., Curtis, D., Di Florio, A., Dickerson, F., Freimer, N. B., Goes, F. S., Jia, X., Jones, I., Jones, L., … Neale, B. M. (2022). Exome sequencing in bipolar disorder identifies AKAP11 as a risk gene shared with schizophrenia. *Nature Genetics*, *54*(5), 541–547. https://doi.org/10.1038/s41588-022-01034-x

Pidoux, G., Witczak, O., Jarnæss, E., Myrvold, L., Urlaub, H., Stokka, A. J., Küntziger, T., & Taskén, K. (2011). Optic atrophy 1 is an A-kinase anchoring protein on lipid droplets that mediates adrenergic control of lipolysis. *The EMBO Journal*, *30*(21), 4371–4386. https://doi.org/10.1038/emboj.2011.365

Pohl, C., & Dikic, I. (2019). Cellular quality control by the ubiquitin-proteasome system and autophagy. *Science (New York, N.Y.)*, *366*(6467), 818–822. https://doi.org/10.1126/science.aax3769

Porstmann, T., Santos, C. R., Griffiths, B., Cully, M., Wu, M., Leevers, S., Griffiths, J. R., Chung, Y.-L., & Schulze, A. (2008). SREBP activity is regulated by mTORC1 and contributes to Akt-dependent cell growth. *Cell Metabolism*, *8*(3), 224–236. https://doi.org/10.1016/j.cmet.2008.07.007

Rahman, T., & Lauriello, J. (2016). Schizophrenia: An Overview. *Focus: Journal of Life Long Learning in Psychiatry*, *14*(3), 300–307. https://doi.org/10.1176/appi.focus.20160006

Rehman, S., Rahimi, N., & Dimri, M. (2024). Biochemistry, G Protein Coupled Receptors. In *StatPearls*. StatPearls Publishing. http://www.ncbi.nlm.nih.gov/books/NBK518966/

Robitaille, A. M., Christen, S., Shimobayashi, M., Cornu, M., Fava, L. L., Moes, S., Prescianotto-Baschong, C., Sauer, U., Jenoe, P., & Hall, M. N. (2013). Quantitative phosphoproteomics reveal mTORC1 activates de novo pyrimidine synthesis. *Science (New York, N.Y.)*, *339*(6125), 1320–1323. https://doi.org/10.1126/science.1228771

Sancak, Y., Peterson, T. R., Shaul, Y. D., Lindquist, R. A., Thoreen, C. C., Bar-Peled, L., & Sabatini, D. M. (2008). The Rag GTPases bind raptor and mediate amino acid signaling to mTORC1. *Science (New York, N.Y.)*, *320*(5882), 1496–1501. https://doi.org/10.1126/science.1157535

Sarraf, S. A., Shah, H. V., Kanfer, G., Pickrell, A. M., Holtzclaw, L. A., Ward, M. E., & Youle, R. J. (2020). Loss of TAX1BP1-Directed Autophagy Results in Protein Aggregate Accumulation in the Brain. *Molecular Cell*, *80*(5), 779-795.e10. https://doi.org/10.1016/j.molcel.2020.10.041

Saxton, R. A., & Sabatini, D. M. (2017). mTOR Signaling in Growth, Metabolism, and Disease. *Cell*, *168*(6), 960–976. https://doi.org/10.1016/j.cell.2017.02.004

Schillace, R. V., & Scott, J. D. (1999). Association of the type 1 protein phosphatase
PP1 with the A-kinase anchoring protein AKAP220. *Current Biology*, *9*(6), 321–
324. https://doi.org/10.1016/S0960-9822(99)80141-9

Scott, J. D., Dessauer, C. W., & Taskén, K. (2013). Creating Order from Chaos: Cellular
Regulation by Kinase Anchoring. *Annual Review of Pharmacology and
Toxicology*, *53*(1), 187–210. https://doi.org/10.1146/annurev-pharmtox-011112-
140204

Shin, H. R., & Zoncu, R. (2020). The Lysosome at the Intersection of Cellular Growth
and Destruction. *Developmental Cell*, *54*(2), 226–238.
https://doi.org/10.1016/j.devcel.2020.06.010

Singh, T., Poterba, T., Curtis, D., Akil, H., Al Eissa, M., Barchas, J. D., Bass, N., Bigdeli,
T. B., Breen, G., Bromet, E. J., Buckley, P. F., Bunney, W. E., Bybjerg-Grauholm,
J., Byerley, W. F., Chapman, S. B., Chen, W. J., Churchhouse, C., Craddock, N.,
Cusick, C. M., … Daly, M. J. (2022). Rare coding variants in ten genes confer
substantial risk for schizophrenia. *Nature*, *604*(7906), 509–516.
https://doi.org/10.1038/s41586-022-04556-w

Skalhegg, B. S., & Tasken, K. (2000). Specificity in the cAMP/PKA signaling pathway.
Differential expression,regulation, and subcellular localization of subunits of PKA.
Frontiers in Bioscience: A Journal and Virtual Library, *5*, D678-693.
https://doi.org/10.2741/skalhegg

Smith, F. D., Esseltine, J. L., Nygren, P. J., Veesler, D., Byrne, D. P., Vonderach, M.,
Strashnov, I., Eyers, C. E., Eyers, P. A., Langeberg, L. K., & Scott, J. D. (2017).
Local protein kinase A action proceeds through intact holoenzymes. *Science
(New York, N.Y.)*, *356*(6344), 1288–1293.
https://doi.org/10.1126/science.aaj1669

Smith, F. D., Reichow, S. L., Esseltine, J. L., Shi, D., Langeberg, L. K., Scott, J. D., &
Gonen, T. (2013). Intrinsic disorder within an AKAP-protein kinase A complex
guides local substrate phosphorylation. *eLife*, *2*, e01319.
https://doi.org/10.7554/eLife.01319

Stephan, J. S., Yeh, Y.-Y., Ramachandran, V., Deminoff, S. J., & Herman, P. K. (2009).
The Tor and PKA signaling pathways independently target the Atg1/Atg13
protein kinase complex to control autophagy. *Proceedings of the National
Academy of Sciences*, *106*(40), 17049–17054.
https://doi.org/10.1073/pnas.0903316106

Sun, P., Wang, L., Yang, Y., Zhang, C.-Y., Yang, L., Fang, Y., & Li, M. (2022). Common
variants associated with AKAP11 expression confer risk of bipolar disorder.
Asian Journal of Psychiatry, *77*, 103271.
https://doi.org/10.1016/j.ajp.2022.103271

Tanji, C., Yamamoto, H., Yorioka, N., Kohno, N., Kikuchi, K., & Kikuchi, A. (2002). A-Kinase Anchoring Protein AKAP220 Binds to Glycogen Synthase Kinase-3β (GSK-3β) and Mediates Protein Kinase A-dependent Inhibition of GSK-3β*. *Journal of Biological Chemistry*, *277*(40), 36955–36961. https://doi.org/10.1074/jbc.M206210200

Taskén, K., & Aandahl, E. M. (2004). Localized effects of cAMP mediated by distinct routes of protein kinase A. *Physiological Reviews*, *84*(1), 137–167. https://doi.org/10.1152/physrev.00021.2003

Taylor, S. S., Zhang, P., Steichen, J. M., Keshwani, M. M., & Kornev, A. P. (2013). PKA: Lessons Learned after Twenty Years. *Biochimica et Biophysica Acta*, *1834*(7), 1271–1278. https://doi.org/10.1016/j.bbapap.2013.03.007

Tomek, J., & Zaccolo, M. (2023). Compartmentalized cAMP signalling and control of cardiac rhythm. *Philosophical Transactions of the Royal Society of London. Series B, Biological Sciences*, *378*(1879), 20220172. https://doi.org/10.1098/rstb.2022.0172

Turco, E., Fracchiolla, D., & Martens, S. (2020). Recruitment and Activation of the ULK1/Atg1 Kinase Complex in Selective Autophagy. *Journal of Molecular Biology*, *432*(1), 123–134. https://doi.org/10.1016/j.jmb.2019.07.027

Turco, E., Savova, A., Gere, F., Ferrari, L., Romanov, J., Schuschnig, M., & Martens, S. (2021). Reconstitution defines the roles of p62, NBR1 and TAX1BP1 in ubiquitin condensate formation and autophagy initiation. *Nature Communications*, *12*(1), 5212. https://doi.org/10.1038/s41467-021-25572-w

Turco, E., Witt, M., Abert, C., Bock-Bierbaum, T., Su, M.-Y., Trapannone, R., Sztacho, M., Danieli, A., Shi, X., Zaffagnini, G., Gamper, A., Schuschnig, M., Fracchiolla, D., Bernklau, D., Romanov, J., Hartl, M., Hurley, J. H., Daumke, O., & Martens, S. (2019). FIP200 Claw Domain Binding to p62 Promotes Autophagosome Formation at Ubiquitin Condensates. *Molecular Cell*, *74*(2), 330-346.e11. https://doi.org/10.1016/j.molcel.2019.01.035

Valvezan, A. J., & Manning, B. D. (2019). Molecular logic of mTORC1 signalling as a metabolic rheostat. *Nature Metabolism*, *1*(3), 321–333. https://doi.org/10.1038/s42255-019-0038-7

Vargas, J. N. S., Hamasaki, M., Kawabata, T., Youle, R. J., & Yoshimori, T. (2023). The mechanisms and roles of selective autophagy in mammals. *Nature Reviews. Molecular Cell Biology*, *24*(3), 167–185. https://doi.org/10.1038/s41580-022-00542-2

Vargas, J. N. S., Wang, C., Bunker, E., Hao, L., Maric, D., Schiavo, G., Randow, F., & Youle, R. J. (2019). Spatiotemporal Control of ULK1 Activation by NDP52 and TBK1 during Selective Autophagy. *Molecular Cell*, *74*(2), 347-362.e6. https://doi.org/10.1016/j.molcel.2019.02.010

Whiting, J. L., Nygren, P. J., Tunquist, B. J., Langeberg, L. K., Seternes, O.-M., & Scott, J. D. (2015). Protein Kinase A Opposes the Phosphorylation-dependent Recruitment of Glycogen Synthase Kinase 3β to A-kinase Anchoring Protein 220. *The Journal of Biological Chemistry*, *290*(32), 19445–19457. https://doi.org/10.1074/jbc.M115.654822

Whiting, J. L., Ogier, L., Forbush, K. A., Bucko, P., Gopalan, J., Seternes, O.-M., Langeberg, L. K., & Scott, J. D. (2016). AKAP220 manages apical actin networks that coordinate aquaporin-2 location and renal water reabsorption. *Proceedings of the National Academy of Sciences*, *113*(30), E4328–E4337. https://doi.org/10.1073/pnas.1607745113

Wu, J., Brown, S. H. J., von Daake, S., & Taylor, S. S. (2007). PKA Type IIα Holoenzyme Reveals a Combinatorial Strategy for Isoform Diversity. *Science (New York, N.Y.)*, *318*(5848), 274–279. https://doi.org/10.1126/science.1146447

Yamamoto, H., Zhang, S., & Mizushima, N. (2023). Autophagy genes in biology and disease. *Nature Reviews. Genetics*, *24*(6), 382–400. https://doi.org/10.1038/s41576-022-00562-w

Zaffagnini, G., & Martens, S. (2016). Mechanisms of Selective Autophagy. *Journal of Molecular Biology*, *428*(9Part A), 1714–1724. https://doi.org/10.1016/j.jmb.2016.02.004

Zellner, S., Schifferer, M., & Behrends, C. (2021). Systematically defining selective autophagy receptor-specific cargo using autophagosome content profiling. *Molecular Cell*, *81*(6), 1337-1354.e8. https://doi.org/10.1016/j.molcel.2021.01.009

Zhao, X., Nedvetsky, P., Stanchi, F., Vion, A.-C., Popp, O., Zühlke, K., Dittmar, G., Klussmann, E., & Gerhardt, H. (n.d.). Endothelial PKA activity regulates angiogenesis by limiting autophagy through phosphorylation of ATG16L1. *eLife*, *8*, e46380. https://doi.org/10.7554/eLife.46380

Zhou, X., Lee, Y.-K., Li, X., Kim, H., Sanchez-Priego, C., Han, X., Tan, H., Zhou, S., Fu, Y., Purtell, K., Wang, Q., Holstein, G. R., Tang, B., Peng, J., Yang, N., & Yue, Z. (2024). Integrated proteomics reveals autophagy landscape and an autophagy receptor controlling PKA-RI complex homeostasis in neurons. *Nature Communications*, *15*(1), 3113. https://doi.org/10.1038/s41467-024-47440-z

Zhou, Y., Zhou, B., Pache, L., Chang, M., Khodabakhshi, A. H., Tanaseichuk, O., Benner, C., & Chanda, S. K. (2019). Metascape provides a biologist-oriented resource for the analysis of systems-level datasets. *Nature Communications*, *10*(1), 1523. https://doi.org/10.1038/s41467-019-09234-6

Zhou, Z., Liu, J., Fu, T., Wu, P., Peng, C., Gong, X., Wang, Y., Zhang, M., Li, Y., Wang, Y., Xu, X., Li, M., & Pan, L. (2021). Phosphorylation regulates the binding of autophagy receptors to FIP200 Claw domain for selective autophagy initiation.

Nature Communications, 12(1), 1570. https://doi.org/10.1038/s41467-021-21874-1